Experimental study on cometary nucleus activity

Diffusion and sublimation of volatiles through ice dust layers

Carla Tamai

Technische Universiteit Delft

TU Delft

Experimental study on cometary nucleus activity

Diffusion and sublimation of volatiles through ice dust layers

by

Carla Tamai

to obtain the degree of Master of Science

at the Delft University of Technology,

to be defended publicly on Monday July 18, 2022 at 9:00 AM.

Student number:	5384508	
Project duration:	January 17, 2022 – July 18, 2022	
Thesis committee:	Prof. Dr. Stéphanie Cazaux,	TU Delft, supervisor
	Prof. Dr. Wouter van der Wal,	TU Delft, chair
	Prof. Dr. Jasper Bouwmeester,	TU Delft, examiner

Cover image retrieved from https://unsplash.com/collections/1147133/stardust

This thesis is confidential and cannot be made public until August 31, 2023.

TU Delft

Preface

As I am approaching the end of the Master here at TuDelft, I feel like I have to stop for a few minutes the drafting of the thesis, and dedicate some words, attention and reward to the people that made it possible.

It goes without saying that it would have been impossible to come to the end without the incredibly helpful support of my supervisor, Stephanie. I remember I did not even start the Planetary Sciences I course that I was already signing your name on a notebook, in order to remember your name and text you as soon as I should have done, to be able to do the thesis with you. After the lesson you gave on meteorites, I knew it was the best decision I could have ever taken. I enjoyed working with you, since the beginning of the Literature Study. I was able to learn a lot, without feeling the pressure, and to be free and choose what I mostly liked for the thesis. Thank you for your, always very rapid, availability and desire to do the best for me, and get me where I aspire. Your advice for the future, your curiosity for Physics and your passion for Space have been the guide throughout this journey. Merci :)

Claramente, Stephanie no fue la unica supervisora que yo tenia. Antes de todo, Belen, gracias por el ayudo, la disponibilidad, apoyo, amistad y tiempo que me has dedicado en los primer tres mesis de esto tfm. Fue un placer trabajar contigo, tomar el cafe con las galletas de tu colega, reir sobre algunos inexplicables resultados que nos salieron algunas veces, o cuando teniamos que llenar el tanque de liquid nitrogen, y por hacerme aprender el español rapidamente, pero sobre todo, gracias porqué creo que en tre meses he aprendido mas que en un año en la Universidad. A seguir, aunque nunca personalmente, gracias Miguel Angel, porque sin ti, algunos resultados seguirían sin sentido. Me encataba cada vez, en las nuestras reuniones, como tu tenias la capacidad de interesarse en cada pequeño detalle y buscar la razon detras de ellos. Gracias porqué con ustedes, los tres meses volaron. Ya vuestros consejos se echan de menos.

Grazie alla mia famiglia, a mia mamma, mio fratello, mia nonna, mio papà e mio nonno, perchè sono stati la consolazione con i ”pacchi da giù”, il supporto e la presenza, seppur da lontano, nei momenti più difficili, la boccata d’aria fresca nelle poche vacanze che ho avuto, l’amore che non hanno fatto mai mancare, i consigli per le scelte del futuro, e il supporto, non solo emotivo, con il quale son potuta arrivare fino a qui e sul quale so di poter contare fino alla fine, per inseguire i miei sogni e la mia felicità. Grazie, da cotti.

E’ pur vero, però, che dietro le quinte ci siete voi, i miei amici, quelli di sempre, e quelli di dopo, ma pur sempre veri. C’è chi viaggia con me su questo razzo (e non treno, perchè sono un ca... di Dottore Magistrale in Ingegneria Aerospaziale ora, lol) della vita dalle elementari, chi dal liceo, chi dalla triennale, chi da Madrid, and some from the amazing experience here in Delft, in and outside the TSH and Campus. To any of you, thank you so so much for lifting up my mood when I needed, for believing in me when I had zero willingness to do so, for the videocalls, the advices, the immense support, for the cakes at TSH, the drinks and Sangria at 6pm, the shopping in Amsterdam ’cause: ”we need a break”, the parmigiana on a Sunday lunch, the days spent yelling at an assignment, the ”copy paste” attitude, the house-hunting, la casa con 4 amici da napoli, l’abbraccio in stazione, la torta de queso en familia, los partidos del Atletico de Madrid, el cachopo, mi amiga chilena, las risas por las calles de Madrid, la pizza di Dominos e il ben and jerry: ”perchè ce lo siamo meritate”, the apple cake in BesteenMarkt, the dinners with the ribs, the bbqs at the lake, the internship at NLR, Ilja and Minoes, Aswin, and everyone that I might be forgetting now. You have been indispensable for me, because, nothing is achieved by being alone, and I had the best travel friends I could have asked for.

Carla Tamai
Delft, July 2022

Abstract

Comets are relatively small celestial icy bodies that orbit the Sun and are made of dust, rock and frozen gases. When close to the Sun, they warm up and release gases. This desorption of volatiles from comets detains many pieces of information on comets' interiors, as well as the morphology of the ices hidden under the dust.

The aim of this work is to study the sublimation and desorption of water and volatiles from cometary ices. Two sets of experiments have been done, one in a high vacuum chamber setup, and the second one in low vacuum. During the first set, sublimation and desorption of CH_4 through amorphous solid water (ASW) ice, and a layer of indene (C_9H_8, as a proxy for dust grains), during thermal processing, are performed in order to simulate temperature changes occurring in cometary environments. These experiments are performed for pure CH_4, as well as CH_4 layered or mixed with H_2O. At about 30 K and with 1 % of CH_4/H_2O abundance ratio, the ices are deposited and the temperature is increased until (maximum) 200 K with a heating ramp of 1 or 5 K/min. Mass and Infrared (IR) Spectroscopy are used to analyze the results through a Quadrupole Mass Spectrometer (QMS) and Fourier Transform Infrared (FTIR) spectrometry. Moreover, comparisons between small and large scale experiments were deemed necessary, in order to show similarities and differences in between water ice behaviour in different vacuum conditions. Therefore, in a very low vacuum environment (0.8 mbar minimum), the second set of experiments was focused on sublimation of water ice, mainly grown in a freezer or within liquid nitrogen. Different types of water ice have been raised (to mimic the difference between mixed and layered deposition in small scale experiments) and at the end, titanium dioxide is used to recreate impurities and the crust in cometary nucleus.

It has been noticed that depending on the heating ramp and type of deposition, the diffusion of methane varies, in terms of both intensity and desorption temperature, being it lower in intensity and higher in temperature when the mixed structure is considered. The same can be noticed when temperature cycles are applied. However, when a layer of indene is placed on top of a layered structure, the thicker the indene layer the later the desorption of methane happens. Within large scale experiments, instead, it is seen, by studying the ratio of the sublimation rates (with temperature and surface area variations), how more sublimation is generated when water ice grains are created and the temperature is thus higher, with respect to the case of ice particles made with Liquid Nitrogen. Between ice particles and blocks of ice it is clear that the particles lead to a bigger surface area and therefore have a major impact on the sublimation process. When adding cold titanium powder to the ice, the sublimation process is slower than for pure water ice.

Through this study, the desorption patter of volatiles in comets, along their orbit, has been reproduced. Some of the slopes within the patterns have been linked to methane sublimation and water crystallization processes in cometary environments. Their shift in desorption temperature have been, therefore, identified.

Contents

List of Figures

List of Tables

List of Symbols and Abbreviations

α	Condensation coefficient	
ϵ	Emissivity	
ν	desorption pre-exponential factor	
π	Pi number	
ρ	Density	
σ	Stefan-Boltzmann	5.67×10^{-8} W/(m^2 K^4)
A	IR Band Strength	
A_b	Albedo	
A_s	Surface Area	
Ar	Argon	
ASW	Amorphous Solid Water	
AU	Astronomical Units	
C_9H_8	Indene	
C_p	Specific Heat Capacity	
CH_4	Methane	
CO	Carbon monoxide	
CO_2	Carbon dioxide	
CS	Carbon monosulfide	
E_d	Desorption Activation Energy	
$F_\odot$	Solar constant	1.37 × 103 J/(m^2 s)
FTIR	Fourier-Transform InfraRed	
H_2CO	Formaldehyde	
H_2O	Water	
HCN	Hydrogen cyanide	
HNCO	Isocyanic acid	
HTFD	Hypersonic Tunnel Facility Delft	
IR	Infrared	
KBr	Potassium Bromide	
Kr	Krypton	
L	Layer thickness	
m_g	mass of the gas molecules	
MCT	Mercury-Cadmium-Telluride	
N	Number of Molecules	

N_2	Nitrogen	
NH_3	Ammonia	
O_2	Dioxygen	
OH	Hydroxide	
P_1	First desorption peak	
P_2	Second desorption peak	
P_3	Third desorption peak	
P_g	Pressure of the gas	
QMS	Quadrupole Mass Spectrometer	
R	Gas constant	8.314 J/(K mol)
$r_{\odot_{AU}}$	Distance between object and Sun in AU	
SCCM	Standard Cubic Centimeters per Minute	
Si	Silicon	
T_g	Temperature of the gas	
T_s	Temperature of the substrate	
T_{eq}	Equilibrium Temperature	
T_{peak}	Temperature of the desorption peak	
TiO_2	Titanium	
TPD	Temperature Programmed Desorption	
UV	Ultra-violet	
Xe	Xenon	

1

Introduction

Comets have always fascinated humans, and nowadays, even though a long way has been made on the topic, as shown, for example, in Festou et al. (2004), still many unresolved issues are present, such as their internal structure and its effect during cometary outbursts. With their unpredictability, bright glowing comae (Combi et al., 2004), substantial crust (Strazzulla, 1999) and their long dust and ion tails (De Pater and Lissauer, 2015), comets are among the most spectacular objects in Space. More than everything, however, it is their evolution and thus internal ice morphology, and orbital behaviour that arouse everyone's curiosity because of their uniqueness, and that are thus here treated.

Water (H_2O) ice is a major constituent of comets, together with dust and many volatiles such as CH_4, which is one of the most common and abundant one, as discussed in Bockelée-Morvan et al. (2004). Many experiments with these two molecules have indeed been performed when studying comets. For example, in Maté et al. (2020), the diffusion of CH_4 in Amorphous Solid Water (ASW) was analysed with the aim to provide diffusion coefficients of CH_4 on amorphous solid water and to understand how they are affected by the ASW structure. On a similar point of view, studies described in Alan May R. (2013a) and Alan May R. (2013b) analyze the release of trapped gases such as Ar, Kr, Xe, CH_4, N_2, O_2, and CO from ASW, both with a crystallization-induced mechanism and as a function, for example, of composition and multi-layer thickness.

When studying comets, therefore, it is impossible not to consider water morphology and its characteristics depending on the type of ice present. Therefore, studies from Jenniskens and Blake (1994), Jenniskens et al. (1995), Jenniskens and Blake (1996) and Mastrapa et al. (2009) have been taken into account. The focus is, for example, on the influence that the astrophysical environment has on the transition from amorphous to crystalline, all its transformation of phases and its band strength along the variations. The behaviour of water in post perihelion passages is also analysed in Stern et al. (1999), Hansen et al. (2016) and Biver, Bockelée-Morvan, Colom, Crovisier, Germain, et al. (1997), which are used as reference articles for this topic. In Snodgrass et al. (2016) the post-perihelion gas production is also analysed. With respect to the other volatiles present in comets, such as CH_4, studies have been conducted on their desorption patter when close to the Sun. An example is in Biver, Bockelee-Morvan, et al. (1997), Rubin et al. (2020) or Biver et al. (2002) on both Comet Hale Bopp and 67P/Churyumov-Gerasimenko. However, from all these papers, a more in-depth explanation of what the different slopes in desorption patters mean is missing.

Many experiments have been performed to deepen the knowledge on the morphology and ices evolution in comets. Some of these studies focused on either the effect of porosity on the rate of outgassing of porous granular ice (Kossacki, 2021), or the adsorption, desorption, trapping, and release of volatile gases by amorphous solid water (Ayotte et al., 2001). Others' studies focus on the influence that molecules such as carbon monoxide and dioxide, methane, and ammonia have on the sublimation of water vapour and thus its sublimation coefficient (Kossacki et al., 2017), or the migration of water through the outer ice layers of a comet till the upper ones, as in Pat-El et al. (2009). Even in Mispelaer et al. (2013), thermal diffusion of H_2CO, NH_3, HNCO, and CO in amorphous water ice was investi-

gated. However the attention was mainly on surface diffusion coefficients and the influence that the temperature in the ASW ice has on them.

In the past, the interest was also on the temperature dependent sublimation properties of hexagonal water ice and the gas diffusion through a dry dust layer covering the ice surface (Gundlach et al., 2011). However, since more information was needed regarding dust layer on top of the ices, the study on the thermal conductivity of porous dust aggregates, from Krause et al. (2011), was investigated and conclusions were taken into account for different volume filling factors of the porous dust samples.

In Collings et al. (2004) and Brown and Bolina (2007) studies were, respectively, on the thermal desorption of 16 astrophysically relevant species through amorphous solid water. On the other hand, a different approach on the study on diffusion of volatiles in ASW has been taken by He et al. (2018). By studying the change in band strength and position of mid-infrared features of OH dangling bonds as molecules move through pores and channels of the water ice, the diffusion of simple molecules have been studied. In Minissale et al. (2022) they also analysed the influence that different parameters, such as the binding energy, have on desorption of interstellar ices. The study is mainly focused on pure ices, but very useful for the study presented here are the experiments on mixed ices (such as Marboeuf et al. (2012)), which are astronomically more realistic and relevant.

Therefore, as noticed from all the previous papers, not many variations to some fundamental cometary parameters, such as the stoichiometry ratio between water and a cometary volatile, the heating rate, the internal structure of the ice and a crust on the surface, have been done, when studying the desorption of a volatile through ASW ice and a layer of dust. In Martín-Doménech et al. (2014), for example, a very similar study to the one presented here has been performed but none of the parameters aforementioned have been changed. They only reproduced the warming up of circumstellar ices and connected it to cometary evolution. Questions on how these parameters influence the desorption of volatiles in astrophysical environments are risen. Therefore, in this project, it is presented how a simplified model of comets, with only methane, water and a layer of indene, behaves along the orbit, during thermal processing, when these parameters are changed. The experiments are performed in a vacuum chamber in order to recreate the conditions in space. Works that have been used to retrieve information on the interaction between water and methane ices and their spectroscopic effects are, respectively, Herrero et al. (2010) and Gálvez et al. (2009).

Moreover, none of the aforementioned works has ever investigated on the difference in the outcome between small and large scale experiments. The latter would be performed in a low vacuum environment, and would, in the same way, consider and study the sublimation and desorption of cometary ices. It is, therefore, for this reason that in this work experiments with mainly water ice, and in the last stages, titanium dioxide, have been performed, at about 0.8 mbar. These tests have the aim to deepen the knowledge and investigate more on the behaviour of water ice with and without impurities in low vacuum conditions, taking into account different amorphous ice structures and changes of phases of the ice. In addition to this, they have been used to compare the results with respect to those from small scale tests, in a high vacuum environment, and see whether any difference would have come out.

1.1. Research Questions

According to what has been explored in the introduction, there is still missing information on comets, their internal morphology, their internal processes and their behaviour when close to the Sun. Therefore, the following research questions have been formulated.

1. How does the internal morphology of cometary nuclei influence the desorption/sublimation of both volatiles and water?
2. How does the heating ramp, along the orbit of a comet, influence the way in which such species desorb and sublimate?
3. What is the influence of the crust on the desorption and sublimation of such species from the inside of cometary nucleus?
4. Does the desorption of methane and water change when two temperature cycles are performed?
5. How does the morphology of water ice change the sublimation process?

6. How does the presence of impurities (for example, titanium dioxide) influence the sublimation of water ice?

1.2. Report Outline

The research and findings of this thesis have been documented in the form of a journal article, included in chapter 2. The conclusions and recommendations for future work are provided in chapter 3. In appendix A and B additional work and calculations performed in Madrid, not inserted in the paper, are presented, and in appendix C and D the second phase of the research project, performed in Delft, is shown.

2

Journal Article

The research work here presented has been documented in the form of a scientific paper, to be submitted to the journal Astronomy and Astrophysics (A&A). The article is provided in this chapter, following the standard A&A template and guidelines.

For consistency in the format, Appendix A (Journal Clarifications and Extensions) and Appendix B (Additional experiments from phase 1 in Madrid), which will not be submitted for publication, have been included to conclude and expand on the work performed in Madrid.

Astronomy & Astrophysics manuscript no. output
July 3, 2022

Laboratory experiments on diffusion and sublimation of methane through ice dust layers to mimic cometary nucleus activity.

Carla Tamai[1], Belén Maté[2], Stéphanie Cazaux[1,3], and Miguel Ángel Satorre[4]

[1] Faculty of Aerospace Engineering, Delft University of Technology, Delft, The Netherlands
e-mail: c.tamai@student.tudelft.nl, carla.tamai@libero.it
[2] Instituto de Estructura de la Materia, IEM-CSIC, Calle Serrano 121, 28006 Madrid, Spain
e-mail: belen.mate@csic.es
[3] Leiden Observatory, Leiden University, P.O. Box 9513, NL 2300 RA Leiden, The Netherlands
e-mail: s.m.cazaux@tudelft.nl
[4] Escuela Politécnica Superior de Alcoy, Universitat Politècnica de València, 03801 Alicante, Spain
e-mail: msatorre@fis.upv.es

Received ; accepted

ABSTRACT

Context. Comets are relatively small celestial icy bodies that orbit the Sun and are made of dust, rock and frozen gases. When close to the Sun, they warm up and release gases. This desorption of volatiles from comets detains many pieces of information on comets' interiors, as well as the morphology of the ices hidden under the dust.
Aims. The aim of this work is to study the sublimation and desorption of CH_4 through amorphous solid water (ASW), and a layer of indene (as a proxy of a layer of crust), during thermal processing, in order to simulate conditions close to cometary environments and temperatures cycles.
Methods. Sublimation and diffusion experiments are performed for pure CH_4, as well as CH_4 layered and mixed with H_2O. At about 30 K and at about 1 % of CH_4/H_2O abundance ratio, the ices are deposited and thermal processes till (maximum) 200 K with a heating ramp of either 1 or 5 K/min are initiated. Mass (Temperature Programmed Desorption, TPD) and Infrared (IR) Spectroscopy are used to analyze the results through a Quadrupole Mass Spectrometer (QMS) and Fourier Transform Infrared (FTIR) spectrometry.
Results. It has been noticed that depending on the heating ramp and type of deposition, the diffusion of methane varies, in terms of both intensity and desorption temperature, being it lower in intensity and higher in temperature when the mixed structure is considered. CH_4 desorbs in multiple steps (three desorption peaks at around, respectively, 50, 140 and 170 K) while water only does it after its change of phase from amorphous to crystalline at about 170 K. The same can be noticed when temperature cycles are applied. However, when a layer of indene is placed on top of a layered structure, the thicker the indene layer the later the desorption of methane happens, but with much more intensity for the first desorption peak, and much less for the third (and last) one.
Conclusions. It is concluded that the characteristics of desorption of methane change with the heating ramp. For a faster ramp, the desorption occurs at higher temperatures, both for mixed and layered deposited ices. On the other hand, when the heating ramp is fixed and the type of ice deposition changes (from layered to mixed), it can be observed that more methane is trapped at low temperature and more comes out once water has sublimated. When a layer of dust/crust is added, a higher temperature is needed for methane to desorb through ASW, even though, in a larger quantity. When temperature cycles are performed, instead, mixed ices will bring to a slower crystallization of water ice and methane sublimation. Through this study, not only the desorption patter of volatiles in comets, along their orbit, has been reproduced but they have also been identified the water crystallization and methane sublimation temperatures in cometary environments.

Key words. Diffusion, Comets: general, Methods: laboratory: molecular, Techniques: spectroscopic

1. Introduction

Comets have always fascinated humans, and nowadays, even though a long way has been made on the topic, as shown, for example, in Festou et al. (2004), still many unresolved issues are present, such as their internal structure and its effect during cometary outbursts. With their unpredictability, bright glowing comae (Combi et al. 2004), substantial crust (Strazzulla 1999) and their long dust and ion tails (De Pater & Lissauer 2015), comets are among the most spectacular objects in Space. More than everything, however, it is their evolution and thus internal ice morphology, and orbital behaviour that arouse everyone's curiosity because of their uniqueness, and that are thus here treated.

Water (H_2O) ice is a major constituent of comets, together with dust and many volatiles such as CH_4, which is one of the most common and abundant one, as discussed in Bockelée-Morvan et al. (2004). Many experiments with these two molecules have indeed been performed when studying comets. For example, in Maté et al. (2020), the diffusion of CH_4 in ASW was analysed with the aim to provide diffusion coefficients of CH_4 on amorphous solid water and to understand how they are affected by the ASW structure. On a similar point of view, studies described in Alan May R. (2013a) and Alan May R. (2013b) analyze the release of trapped gases such as Ar, Kr, Xe, CH_4, N_2, O_2, and CO from ASW, both with a crystallization-induced mechanism and as a function, for example, of composition and multi-layer thickness.

6

When studying comets, therefore, it is impossible not to consider water morphology and its characteristics depending on the type of ice present. Therefore, studies from Jenniskens & Blake (1994), Jenniskens et al. (1995), Jenniskens & Blake (1996) and Mastrapa et al. (2009) have been taken into account. The focus is, for example, on the influence that the astrophysical environment has on the transition from amorphous to crystalline, all its transformation of phases and its band strength along the variations. The behaviour of water in post perihelion passages is also analysed in Stern et al. (1999), Hansen et al. (2016) and Biver et al. (1997b), which are used as reference articles for this topic. In Snodgrass et al. (2016) the post-perihelion gas production is also analysed. With respect to the other volatiles present in comets, such as CH_4, studies have been conducted on their desorption patter when close to the Sun. An example is in Biver et al. (1997a), Rubin et al. (2020) or Biver et al. (2002) on both Comet Hale Bopp and 67P/Churyumov-Gerasimenko. However, from all these papers, a more in-depth explanation of what the different slopes in desorption patters mean is missing.

Many experiments have been performed to deepen the knowledge on the morphology and ices evolution in comets. Some of these studies focused on either the effect of porosity on the rate of outgassing of porous granular ice (Kossacki 2021), or the adsorption, desorption, trapping, and release of volatile gases by amorphous solid water (Ayotte et al. 2001). Others' studies focus on the influence that molecules such as carbon monoxide and dioxide, methane, and ammonia have on the sublimation of water vapour and thus its sublimation coefficient (Kossacki et al. 2017), or the migration of water through the outer ice layers of a comet till the upper ones, as in Pat-El et al. (2009). Even in Mispelaer et al. (2013), thermal diffusion of H_2CO, NH_3, HNCO, and CO in amorphous water ice was investigated. However the attention was mainly on surface diffusion coefficients and the influence that the temperature in the ASW ice has on them.

In the past, the interest was also on the temperature dependent sublimation properties of hexagonal water ice and the gas diffusion through a dry dust layer covering the ice surface (Gundlach et al. 2011). However, since more information was needed regarding dust layer on top of the ices, the study on the thermal conductivity of porous dust aggregates, from Krause et al. (2011), was investigated and conclusions were taken into account for different volume filling factors of the porous dust samples.

In Collings et al. (2004) and Brown & Bolina (2007) studies were, respectively, on the thermal desorption of 16 astrophysically relevant species through amorphous solid water. On the other hand, a different approach on the study on diffusion of volatiles in ASW has been taken by He et al. (2018). By studying the change in band strength and position of mid-infrared features of OH dangling bonds as molecules move through pores and channels of the water ice, the diffusion of simple molecules have been studied. In Minissale et al. (2022) they also analysed the influence that different parameters, such as the binding energy, have on desorption of interstellar ices. The study is mainly focused on pure ices, but very useful for the study presented here are the experiments on mixed ices (such as Marboeuf et al. (2012)), which are astronomically more realistic and relevant.

Therefore, as noticed from all the previous papers, not many variations to some fundamental cometary parameters, such as the stoichiometry ratio between water and a cometary volatile, the heating rate, the internal structure of the ice and a crust on the surface, have been done, when studying the desorption of a volatile through ASW ice and a layer of dust. In Martín-Doménech et al. (2014), for example, a very similar study to the one presented here has been performed but none of the parameters aforementioned have been changed. They only reproduced the warming up of circumstellar ices and connected it to cometary evolution. Questions on how these parameters influence the desorption of volatiles in astrophysical environments are risen. Therefore, in this paper, it is presented how a simplified model of comets, with only methane, water and a layer of indene, behaves along the orbit, during thermal processing, when these parameters are changed. The experiments are performed in a vacuum chamber in order to recreate the conditions in space. Works that have been used to retrieve information on the interaction between water and methane ices and their spectroscopic effects are, respectively, Herrero et al. (2010) and Gálvez et al. (2009).

In section 2 and 3, respectively, the experimental set up and procedure, for the experiments, are described. In section 4 the results and the discussion are presented divided in subsections on the effect of the variations of both the heating ramp and the type of deposition on the desorption of methane through ASW ice, on temperature cycles, water ice morphology and effect of the crust on the desorption of methane. Following, the conclusions are reported in section 5.

2. Experimental Setup

The set up has been previously described in Maté et al. (2021). However, a new cryostat, the ARS DE-204AB, has been installed on top of the high vacuum chamber. The temperature is controlled with a thermofoil heater and, at the end of the cold head, a silicon diode that, with a Lakeshore temperature controller, can give an accuracy of 0.5 K at the end tip between 10 and 300 K. A linear heating ramp with a rate up to 6 K/min can be performed with this system. In the cold head a sample holder made in copper is placed. It is designed so that the sample can be studied in transmission configuration. A Si wafer, of 25 mm diameter and 1 mm thickness, is allocated on the holder leaving an exposed surface of a circle of 10 mm diameter. With this system, the end tip can reach 10 K within 45 minutes.

The vacuum system can reach a background pressure in the 10^{-8} mbar range at room temperature and can get to 10^{-9} mbar with the cryostat on. The chamber is linked to a Bruker Vertex70 FTIR spectrometer through KBr windows and the sample will be able to face the IR beam of the spectrometer thanks to a rotatable flange that allows the holder to change its orientation. Different sets of experiments are performed but for all of them, mainly water, methane, and indene in some cases, are deposited at 30 K. Sometimes they are mixed and sometimes layered, but in both cases they are warmed, with a heating ramp of 5 or 1 K/min, till 140 K or 200 K, to reproduce the conditions and behaviour of comets when they are along their orbit and close to perihelion. The heating ramp of 5 K/min is chosen because it is close to the fastest ramp provided by the set up in order to do comparisons, and the 1 K/min ramp is chosen as the slowest one to perform reliable thermal programmed desorption experiments. At lower rates, the contamination of the ices due to the background pressure in the high-vacuum chamber could become significant.

In order to introduce gaseous methane in the vacuum chamber, an independent line equipped with a 2 Standard Cubic Centimeters per Minute (SCCM) mass flow controller is used, as

described in Molpeceres et al. (2017). On the other hand, the gas flow of distilled water is controlled with a leak valve (Maté et al. 2020) and introduced in the chamber through another independent line. The water that is introduced is three times freeze-pump-thawed. This line is heated to avoid condensation. The gases will then deposit forming two ice layers of the same thickness, on the two sides of the IR transparent Si substrate. At 10 cm below the end of the cryostat's cold finger, in the vacuum chamber, there is the inlet port for the two independent gas lines (see Figure 1). These lines are directed towards the chamber walls, in such a way that all the molecules of the gas fill the chamber for background deposition.

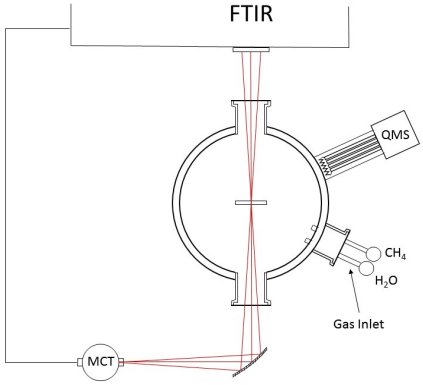

Fig. 1. IR Spectroscopy measurements' setup.

Infrared spectra are here recorded through a transmission configuration thanks to the FTIR spectrometer, provided with a Globar source, a KBr beamsplitter and a MCT Wide liquid nitrogen detector. The accumulation scans for this work vary depending on the heating ramp used, and more precisely, they are 100 if the ramp is 5 K/min, 300 for a 1 K/min ramp, and 500 scans for the background. The resolution used is 4 cm^{-1}, with an aperture of 4 mm.

The number of molecules present in the ices grown has been determined via the IR absorbance spectra ($Abs(v)$) and IR band strengths (A), that allowed to compute the stoichiometry ratio in the ice mixtures. The OH-stretching (symmetric and asymmetric) band at 3200 cm^{-1} for water and the v_4 bending mode at 1300 cm^{-1} for methane are taken into account. For the experiments with indene, the most intense band is taken into account, which is at 760 cm^{-1}. The absorption coefficients are A_{3200}= 2×10^{-16} cm $molec^{-1}$ (Mastrapa et al. 2009), A_{1300}= 7×10^{-18} cm $molec^{-1}$ (Molpeceres et al. 2017) (we assume that the water ice density remains constant to do comparisons with Mastrapa et al. (2009) despite it is known it varies with T), and A_{760}=2×10^{-17} cm $molec^{-1}$ (reference to be published by B. Maté). Therefore, the stoichiometry is given by the ratio between the number of molecules of methane and the number of molecules of water. This number of molecules N is given by:

$$N = \frac{\int Abs(v)dv}{A} \quad (1)$$

where the integral extends over an IR band.

The stoichiometry ratio is obtained by $\frac{N_{met}}{N_{wat}}$ and is put in percentage.

Moreover, to obtain the ice layer thickness (L), the formula adopted is:

$$\rho = \frac{N}{L} -> L = \frac{N}{\rho} \quad (2)$$

The density, ρ, is expressed in molecules/cm^3. Its starting values for deposition of the ice mixtures at 30 K are: ρ_{CH_4}=0.46 g/cm^3 (Molpeceres et al. 2017) and ρ_{H_2O}=0.65 g/cm^3 (Dohnálek et al. 2003). Regarding indene, since there is no published value for its density at the solid phase, the one of the liquid is assumed in this paper, and it is $\rho_{C_9H_8}$=0.997 g/cm^3 (Linstrom & Mallard 2001).

In the case the (mixed) ice at 30 K is formed by co-deposition of both methane and water, the measurement of the thickness of the ice is less accurate because the band strengths for the specific mixed system are not known. However, considering the same values as for the pure species, there is an error of the order of 10 % (Kerkhof et al. 1999).

By following this method, for every experiment performed, around the same thickness has been obtained for methane and water and it is, respectively, around 10 and 600 nm.

The software programs that are used to analyze the results in the laboratory are OPUS and MasSoft. The first one is a spectroscopy software that helps to evaluate, measure, analyze and process IR Spectra. MasSoft is, on the other hand, a software for mass spectrometer control and data manipulation. In order to better present and study the results, however, ORIGIN was used. It is a data analysis and graphing software used with regards to science and engineering.

3. Experimental Procedure

The procedure followed here has been similar throughout the entire duration of the research and only small differences for some specific cases are added. The general idea is to study methane and water in different configurations to see how their desorption change depending on different factors. The two molecules were either deposited in layers or mixed, keeping always the same stoichiometry ratio around 1 %. During most of the experiments a heating ramp (of either 1 or 5 K/min) from 30 K to 200 K was applied. In some specific experiments a top layer of indene was added, and in few final cases temperature cycles (warm up and cool down) were performed from 30 to 140 K. The stratification of the nucleus of comets is considered in this study in such a way that temperature cycles are analysed for lower parts of the nucleus where the temperature does not reach 200 K, even if at perihelion, due to the presence of other external layers.

The first step, of all the experiments, was to deposit always the two molecules, methane and water. For a layered structure, first CH_4 and then H_2O have been deposited sequentially, while for the mixed one both of them have been simultaneously deposited, and in both cases, at 30 K. For 1 % ratio of methane over water, as it can be found in comets, and a layered structure, several seconds of deposition have been applied for the deposition of methane and several minutes for water, filling the chamber with a pressure in the 10^{-5} range for both gases. When considering a mixed configuration instead, in order to have the same stoichiometry ratio, the valves for the inlet pressure of water and the set point for methane are changed so that with a different pressure (and deposition time) the right amount of methane and

water would have been deposited. Therefore, it was computed that several seconds were necessary for the co-deposition, with a pressure in the chamber of around 10^{-4} mbar.

After deposition, a heating ramp of either 1 or 5 K/min is applied, starting from 30 K until a temperature of 200 K. During the warming up, the effects of the different factors such as different ramp, and different type of deposition are observed. When 200 K are reached, the experiment is stopped.

Moreover, to mimic the crust of comets C_9H_8, a less volatile material, is added on top of the ice mixture. It has been reported that the crust of the comets is made out of ammonium salts, apart from processed materials by cosmic rays, dust, non-volatile and organic materials (Strazzulla 1999). Since it is not possible in this laboratory to reproduce this crust, indene is used, which has, as for the dust, a sublimation temperature which is higher (around 180 K) than the one of water (which, instead, is around 170 K), in such a way that it stays on the surface at least till desorption of water, influencing it. To determine the effects of the thickness of the crust on the desorption of methane, different deposition times of indene were adopted (10, 30, and 60 minutes), at a temperature of 30 K. By using the IR spectra and the band strength mentioned in the previous section, the number of molecules of indene deposited are computed. Moreover, by assuming the density of indene the same as the one at its liquid phase, the following thicknesses are obtained for, respectively, 10, 30 and 60 min of deposition: 25 nm, 78 nm and 108 nm.

When temperature cycles are realized in the laboratory, they were not stopped at 200 K but at 140 K, and, by using the same ramp, the system is cooled down again to 30 K, warmed up another time to 140 K, and finally got back to the initial conditions of 30 K.

4. Results

When a Temperature Programmed Desorption (TPD) of an ice mixture of methane and water is performed from 30 K to 200 K, three desorption peaks (as also reported in Collings et al. (2004)) appear for methane: one around 50 K (P_1), one around 140 K (P_2) and another one between 160 and 180 K (P_3), while one peak appear for water, at around 170 K, due to water sublimation (Figure 2).

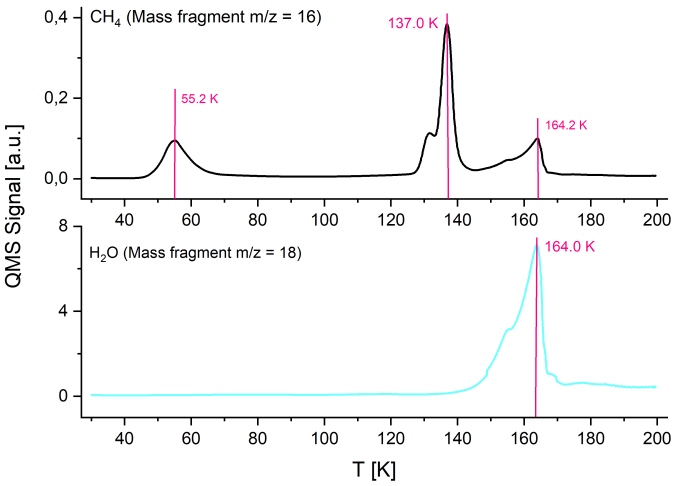

Fig. 2. QMS signal for both CH_4 and H_2O with respect to temperature, for a layered structure, a 1 % stoichiometry ratio and a 1 K/min heating ramp.

The three peaks for methane are due to the following:

1. P_1: Sublimation temperature of low interacting methane (with water) occurs around 60 K. In this first desorption peak not all methane desorbs because it is, in part, either trapped inside or below the water ice.
2. P_2: Crystallization of water and thus sublimation of methane occurs around 140 K. The transformation phase from amorphous to crystalline happens and methane is pushed out of the water matrix.
3. P_3: Co-desorption with water occurs between 160 and 180 K. The remaining quantity of methane that is still either below or mixed with water ice comes out with it.

The case reported in Figure 2 is used as an example of the behaviour of both methane and water in the type of experiments performed in this study.

Papers from Jenniskens & Blake (1996) and Jenniskens & Blake (1994) report that there are three main different types of water ice between 15 and 188 K, confirming not only the idea that at around 140 K, crystallization into cubic ice starts, as just mentioned, but also that between 40 and 70 K a transition to the low density ASW ice happens and impurities have more opportunity to desorb (first desorption peak of methane, P_1). However, still some amorphous ice is retained when crystallization happens (as explained in 4.2.1) and, for this reason, some impurities are retained and left out during P_3.

4.1. Effect of heating ramp and type of deposition on the desorption of methane through ASW ice

The effects on the desorption of methane through ASW ice of the variation of both the warming ramp and the type of deposition (of both ices) are seen in Figure 3. The latter presents the normalised (with respect to the QMS signal of the 2nd peak) QMS signal of methane versus temperature. It shows experiments with layered ices in the top panel and mixed ices in the bottom one, at different heating ramps. With the black line the 1 K/min ramp case is shown, while with the red one the 5 K/min ramp. In blue and green, respectively for 1 and 5 K/min ramp, pure methane desorption is given.

The pure desorptions of methane are used not only for validation of the following results but also as a comparison with the desorption of mixed ices. The desorption of pure water is not shown because it is not expected to change much in the experiments.

Figure 3 shows the effect of the different heating ramp into the shift in the desorption temperature, that goes along with the results from the simulations of Brown & Bolina (2007). Both for a layered structure and a mixed one, in P_1 and P_3, the faster the ramp the larger the shift to higher temperatures. This is due to the fact that higher ramp leaves less time for the molecules to warm up and thus desorb. Moreover, the binding energies of molecules are directly linked to the temperature of desorption (Minissale et al. 2022). It is known that the binding energy between water and methane is stronger than the one between methane and methane and as a consequence binding energies of CH_4 molecules are stronger in the mixed case than the layered one. This explains why desorption occurs at lower temperatures for the layered case than for the mixed one.

The change of the ramp also influences the desorption temperatures. For a specific temperature, the molecules need a certain

time to desorb. If the ramp is fast, then the time spent per kelvin is low, and the desorption of molecules will shift to higher temperatures, due to the difficulty for the molecules to separate and evaporate.

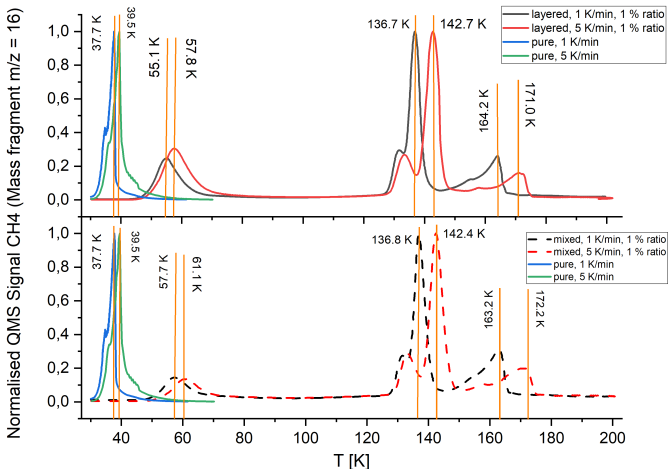

Fig. 3. Normalised QMS signal for CH_4 with respect to temperature, for different heating ramps of the mixture H_2O : CH_4. The mixed cases are indicated with a dashed line, instead the layered ones with a solid line.

It should be noted that methane sublimation temperature can be shifted when mixed with water and pure. In the pure desorption case it sublimates around 40 K and for the other cases at almost 60 K. Such shift in temperature reflects the mobility and binding energy of the CH_4 molecules in the ice.

Also, it can be noticed that the position of the P_2 do not vary with the type of ice deposition, but it does when a different heating ramp is chosen. This is due to the fact that P_2 relates to the crystallization of the water ice, which is not much affected by the small fraction of CH_4 (1 % approx) present in the ice mixtures.

Figure 4 allows a direct comparison between different deposition types regarding layered and mixed ices structure. In the mixed case more methane is trapped in the water ice matrix in P_1, resulting in a lower first peak with respect to the layered case. In the latter, at the beginning it is easier for methane to escape due to its diffusion through the routes made by the pores in the water ice. On the other hand, in P_3, the mixed case shows a higher desorption, due to the higher amount of methane still present in the mixture.

In addition, the temperature of the first peak is lower for layered than mixed case, while on the other hand, for the third peak, the mixed case desorption peak occurs at lower temperatures, with a difference of 1 K. This is because in the layered case, in P_1 methane diffuses through the pores while in the mixed case it is trapped within water ice. On the other hand, in P_3 there is the release of trapped CH_4, which happens at higher temperatures in the layered case, since less methane is present.

In Table 1 all the values of the methane peak ratios (P_1/P_2 and P_3/P_2), for both the layered and the mixed ice structure, are presented. They are all less than 1, leading to the fact that the highest quantity of methane is released during the second peak, linked to the crystallization of water. Looking at the difference between the two ice structures, between cases with the same heating ramp, it is noticed that P_1/P_2 is always larger for the layered case than for the mixed one, while for P_3/P_2 it is always larger for mixed ice. This is in agreement with what previously discussed,

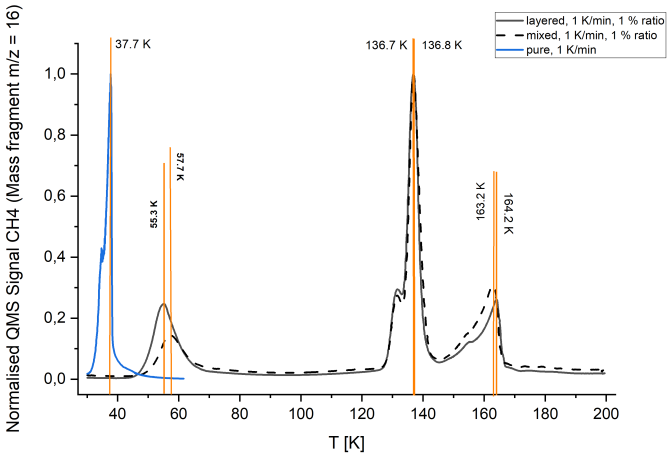

Fig. 4. Normalised QMS signal for CH_4 with respect to temperature, for different deposition types for the mixture H_2O : CH_4. The mixed case is indicated with a dashed line, instead for the layered case the line is solid.

concerning the mixed case within which methane molecules are trapped in water ice at the beginning and from which cannot escape.

Table 1. Different methane peak area ratios for the different experiments performed from QMS.

Ratio	Layered 1 K/min	Mixed 1 K/min	Layered 5 K/min	Mixed 5 K/min
P_1/P_2	0.387	0.249	0.455	0.207
P_3/P_2	0.396	0.487	0.321	0.434

In Figure 5 the IR absorbance spectra of the mixture of water and methane are shown at four different temperatures (30, 80, 150, and 180 K), for one experiment performed (as an example for all the others), which is the one with mixed ices and a heating ramp of 1 K/min. The temperatures taken into account are the deposition temperature at 30 K, and then the ones at the end of each of the three methane desorption peaks (80, 150 and 180 K respectively). This is in order to notice the decrease of methane and water during the heating ramp, and to show its correlation with the TPD previously presented. The QMS seems to be more sensible, with respect to the FTIR, thus leading us to more information. This is due to the fact that the number of CH_4 molecules detectable via absorption IR spectra is related with its IR band strength (A), that is, for methane, quite low (A around 10^{-18} cm/molecule) in comparison with other molecules such as, for example, water (A around 10^{-16} cm/molecule).

In the spectra it is seen that, in accordance with Figure 3 and 4, most of the methane goes out during the second peak, till completely vanish at the end of the third and last peak. The difference between the quantity that desorbs in the first peak with the one that goes out during the second and third peak can be seen in the spectra, and is consistent with results from the QMS. However, methane does not desorb only at these three specific temperatures but also in between them (starting from after the first peak), due to the continuous change in ASW structures during warming up (Jenniskens & Blake 1994). Regarding water the transformation into (different) crystalline phases can be detected. However, for more information see section 4.2.1.

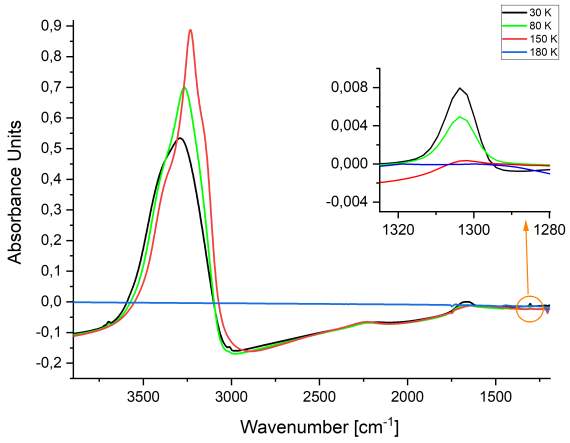

Fig. 5. IR spectra from 3800 cm^{-1} to 1200 cm^{-1} wavenumber for the mixed experiment with a heating ramp of 1 K/min and 1 % ratio stoichiometry, at temperatures of 30, 80, 150 and 180 K.

4.2. Temperature Cycles

In this section we perform identical experiments as before, but this time we carry out two temperature cycles, meaning that the temperature is increased until 140 K, decreased to 30 K, increased again to 140 K and decreased again to 30 K. Such cycles are meant to mimic the thermal evolution of comets during several orbits around the Sun, and to observe their effects on the desorption of both methane and water. This precise type of experiments is mainly to study the behavior of the internal layers of the nucleus of the comet, which do not reach 200 K even at perihelion, and therefore do not immediately desorb from the nucleus of the comet, as the external layer does. In Figure 6 the QMS signal for methane has been represented in order to see that, in this case, after one cycle, still some methane and water are retained. With the black solid line, the layered case is shown, while with the black dashed one, the mixed morphology of the ice is represented. The QMS signal is reported for the four different ramps and therefore the temperature on the x axis increases and decreases depending on the case. Each ramp is delimited by the starting temperature of either 140 or 30 K. In Figure 6 also a zoom on the second heating ramp is reported in order to better show the two methane desorption peaks, and its change of magnitude (from 10^{-7} to 10^{-9} arbitrary units (a.u.)).

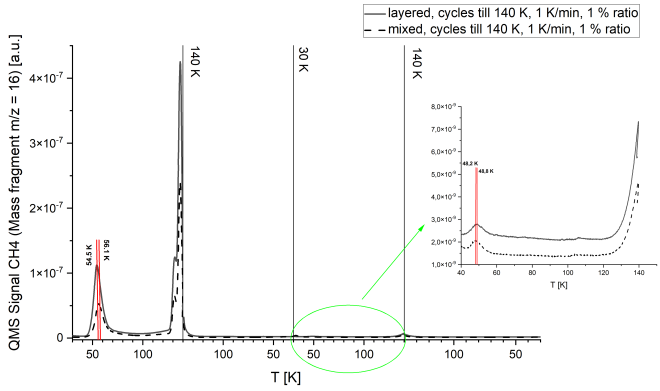

Fig. 6. QMS signal of methane during two temperature cycles for both layered and mixed $H_2O : CH_4$ ice mixtures.

Table 2 indicates, for each cycle and for each ice structure (layered or mixed), the temperatures relative to the methane sublimation peaks. During the second cycle, the desorption peaks for methane occur at lower temperatures than the one of the first cycle (see Table 2). This is because less amount of methane is trapped but it mainly shows the difference of diffusion of methane through amorphous and crystalline water ice. Water molecules reorganize themselves and pushes CH_4 out of its structure, reduces the Van Der Waals interactions and causes sublimation (Maté et al. 2020). The temperature of the first desorption of methane during the first cycle is lower for layered case since it is easier for methane to escape through the routes created by the pores. That same first peak, for the second cycle, occurs before for the mixed case, because a larger quantity needs to be expelled. However, the peaks almost coincide. On the same note, the second methane peaks are very similar since they both show diffusion of methane through crystalline water ice and thus during phase transformation of water. For the aforementioned reason, however, they slightly change between the first and second temperature cycle. Although for methane it is seen a shift, even if small, in the position of both desorption peaks, the same does not happen for water, which, instead, is always starting its crystallization process at around 140 K.

Generally speaking, by looking at the difference between layered and mixed, the methane that desorbs is less for the latter due to the fact that for mixed ices more cycles are needed in order to get a perfect crystalline structure, due to the presence of methane trapped in water. Even though no calculation was performed on the effect of several approaches close to the Sun, in the work by Marboeuf et al. (2012) it does state that mixed ices are more difficult to release trapped volatiles.

Table 2. Temperature of the peaks, from QMS, of methane during two temperature cycles, for both layered and mixed desorptions.

N° cycle	Molecule	Peak point	$T_{layered}$ [K]	T_{mixed} [K]
1st	CH_4	P_1	54.5	56.1
1st	CH_4	P_2	139.7	139.6
2nd	CH_4	P_1	48.8	48.2
2nd	CH_4	P_2	137.1	137.0

In Table 3 the ratio, CH_4/H_2O, of number of molecules in the ice at the end of both the first and the second cycle is reported. At the end of the second cycle, for the layered case, methane is almost fully desorbed. Instead, for the mixed case, a small fraction remains in the ice and will desorb as temperature increases. This is in agreement with what was previously mentioned that a mixed ice needs more cycles to perfectly crystallize. For the same reason, at the end of the first cycle, considering that the ratio between water and methane at the beginning of the cycles is almost the same (see Table 3), a more important fraction of methane is retained for the mixed case. In addition to this, it can be noticed that most of the species desorb during the first cycle, rather than the second one.

Table 3. CH_4/ H_2O number molecule ratios derived from the IR spectra, at 30 K (end of two consecutive temperature cycles) for both experiments performed.

Cycles	Ratio layered	Ratio mixed
beginning	1.3 %	1.1 %
end 1st	0.14 %	0.25 %
end 2nd	0.07 %	0.16 %

4.2.1. Water Ice Morphology

Water is deposited at 30 K and is therefore amorphous. During warming up, the ice transforms into crystalline. The evolution of the water ice spectra during the two warming-cooling cycles is presented in Figure 7. It clearly shows the change of phase during the first heating ramp. The shape of the (blu) spectrum changes, mostly at the end with the very last curve visible in the figure, due to the change of phase from amorphous to crystalline. For the other three ramps (1st decrease, 2nd increase and 2nd decrease, respectively in red, gray and green), the shape of the spectrum does slightly vary from red to green, through gray, reorganizing itself and going into a better crystalline. The bigger changes are, therefore, during the warming up because energy is given to the ice for the molecules to reorganize, and eject the remaining methane. During the last cooling down, no appreciable variation is noticed.

The intensity of the IR water band at 3000 cm^{-1}, computed as its integral in the absorbance spectra, is shown in Figure 8, as a function of temperature, between 30 and 140 K. The integrals for each warming up or cooling down are computed, for both the layered and the mixed case, and then put together in one graph each. The lines/trends shown are obtained by computing, for every spectra recorded by the system, the integral, in the absorbance spectra, of the IR water band at 3000 cm^{-1}. The spectra are recorded every one minute and a half, and at each time, a temperature corresponds. Therefore, the shown graph can be generated by connecting all these points, and "interpolating" them to better observe the trend. Figure 8 has to be read following the arrows from the starting point of the blue line till the ending point of the green line, in such a way to follow the warming up and cooling down of the temperature cycles. After the blue line, which represents the first warming, the red line shows the cooling from 140 K to 30 K, and successively, the gray line for the second warming from 30 K to 140 K, and then the green line for the second and last cooling, from 140 K to 30 K. During the experiment with a layered deposition, the final part of the cooling down was not recorded which is the reason why the line is not entirely available.

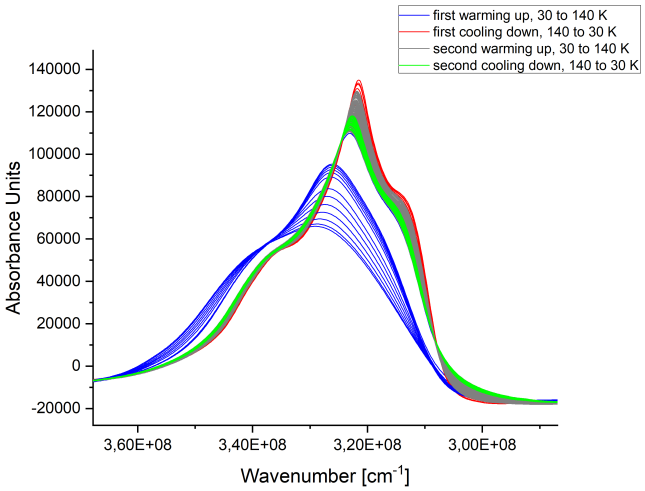

Fig. 7. Infrared spectra of water during the entire duration of two temperature cycles, for the layered ice deposition case.

To better explain Figure 8, an estimation of the amount of water molecules that condensate on top of the ice during the different temperature cycles, due to the residual water pressure present in the high vacuum chamber, has been made. The numbers are given in Table A.1 of appendix A.

When looking at Figure 8, the following can be observed:

- During the first warming up: the intensity of water band increases meaning a change that is mainly due to the transformation of the amorphous ice till its crystallization at 140 K (see Figure 7), although it is also affected by the growing of the ice layer due to the contamination of water molecules inside the vacuum chamber (see Table A.1 in appendix A)
- During the first cooling: there is still an increase in the band due to transformation from crystalline to crystalline cold (Mastrapa et al. 2009). The band changes due to a variation in the IR band strength (as a function of temperature) in crystalline amorphous solid water. In this case the increase in the number of molecules due to contamination is already negligible (see Table A.1 in appendix A).
- During the second warming up, water ice reorganizes itself only in a better crystalline form, without making the trend change. There is not much difference between the red and gray line in Figure 8. Only for larger temperatures a difference can be seen. This is due to the fact that the initial amorphous structure is still not completely crystalline. As it is seen in Jenniskens & Blake (1996) not all water crystallizes and thus still some amorphous one remains, probably due to water itself and the impurities.
- During the second cooling: the water band increases only because of a change in temperature, being already a crystalline cold.

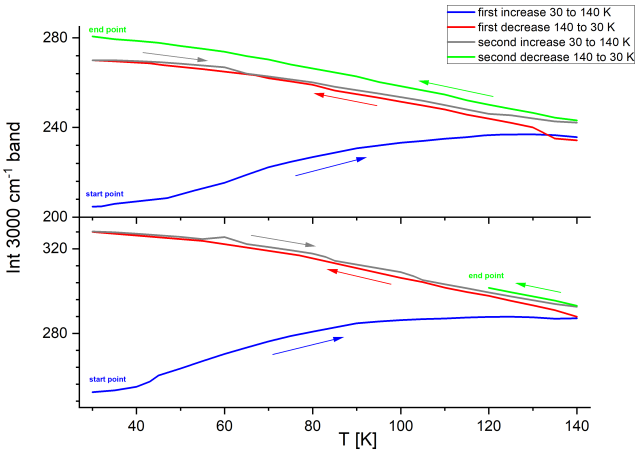

Fig. 8. Integral of water band at 3000 cm^{-1} for both mixed (top panel) and layered (bottom panel) deposition type (stoichiometry ratios of 1 %) during two consecutive temperature cycles, with a ramp of 1 K/min.

4.3. Indene (crust) layer on top of the H_2O : CH_4 mixture

In Figure 9 it can be seen that when adding a layer of indene, on the mixture H_2O : CH_4, the first peak of desorption of methane is shifted to higher temperatures and this temperature increases with increasing crust thickness. This is because methane is retained by the crust and thus higher temperatures are needed to make it diffuse out of the ice.

The intensity with which methane goes out in P_1 increases the more the thickness of the crust increases. This is, assuming the indene as a dust, due to the fact that the normalized rate of

penetrating molecules through a dust layer is inversely proportional to its thickness and therefore the thicker the layer the more molecules go out (Gundlach et al. 2011). This can be explained through the resistivity model (Gundlach et al. 2011) for which a dust layer behaves as if it was a resistor, with respect to the gas flux. In this case, indeed, a huge difference will be made by the diverse specific heat capacity between indene (our dust) and water ice: $C_{p,liquid,indene}$ = 186.9 J/(mol K) (thought to be constant between liquid and frozen form), and $C_{p,liquid,water}$ = 75 J/(mol K) (that is halved when water is frozen). From the aforementioned study, two results are obtained. Either the temperature of the dust layer remains high enough in order to not have any condensation and re-condensation of molecules inside it (Krause et al. 2011), or the temperature of the dust layer is principally cold enough for ice condensation to take place.

The thicker the layer of indene, the higher the temperature at which P_1 appears. Therefore, there is a temperature gradient within the indene layer with the lowest temperature on the surface. The thinner the layer the more methane molecules condensate within the indene, since the lowest temperature of the gradient is still low (as seen in the desorption temperature peak in Figure 9) and thus less methane sublimate as it is observed in Figure 10. What just explained is in agreement with the second hypothesis from Gundlach et al. (2011). On the other hand, the thicker the layer, the higher the lowest temperature of the gradient will be (because of higher desorption temperature peak, as seen in Figure 9) and thus no condensation or re-condensation will happen, bringing to a larger amount of CH_4 desorbed, as explained in Krause et al. (2011) and as the first hypothesis from Gundlach et al. (2011).

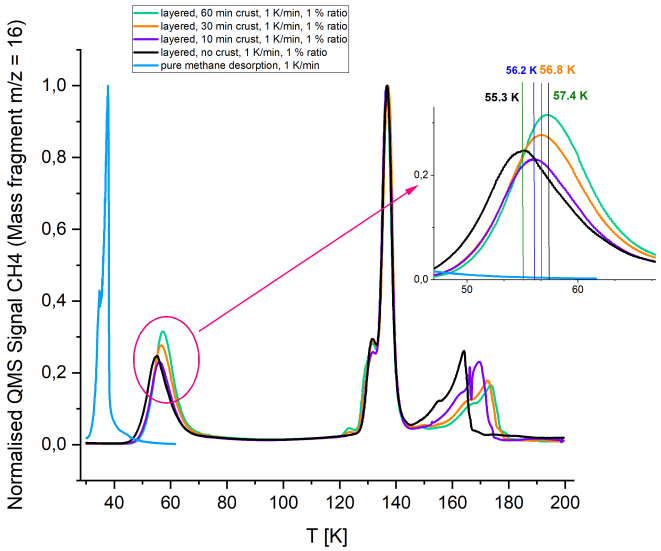

Fig. 9. Normalised QMS signal of methane, with respect to temperature, for different cases of thickness of the indene crust put on top of the H_2O : CH_4 mixture.

For P_3, it is clear that the thicker the crust the less quantity of methane desorbs and this occurs at a higher temperature. Therefore, the shift in the peak is to higher temperatures and has lower intensities, with increasing crust thickness. This means that it is still very difficult for both water and methane to desorb in the presence of a very thick crust. However, this does not mean that methane will not fully sublimate, eventually. On the other hand, this seems to be in accordance with what is seen in P_1, where the thicker the crust the more the methane sublimated, and thus less is left to be diffused at the end of the ramp.

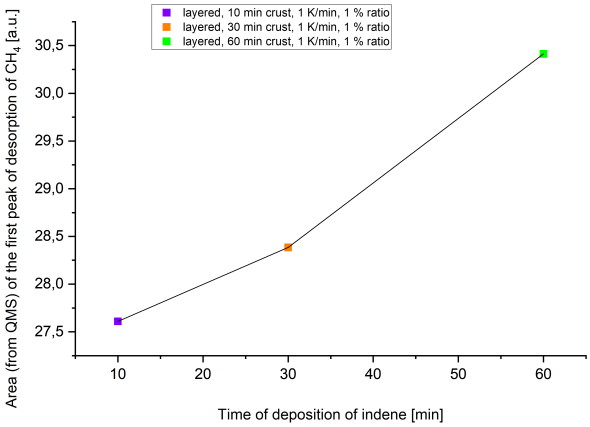

Fig. 10. Area (from QMS) of the first peak of desorption of methane as a function of the quantity of indene put, in terms of deposition time (in min), for the three experiments with indene.

5. Conclusions

The desorption characteristics of methane through amorphous solid water, and a layer of crust, have been studied with thermal programmed desorption through mass and infrared spectroscopy. We considered the abundance ratio of methane in water as it is in the nucleus of comets, a heating ramp that allows to study the evolution of the ices and a deposition type that alternates between layered and mixed.

1. It is observed that when the heating ramp changes, the characteristics of the desorption of methane change too. For a faster ramp, the desorption happens at higher temperatures, both for a mixed and a layered structure. This is due to the conductivity along the ice. The higher the heating ramp, the more difficult it is to have the same temperature in the sensor and in the ice, and even more difficult it is to have the same temperature along the whole ice structure, since it is not a good conductor. Moreover, the shift in temperature is larger in the case of mixed structure, rather than layered one, due to the binding energies, which are stronger in the mixed case. For the latter, when the heating ramp is fixed and the type of ice deposition changes (from layered to mixed), more methane is trapped at low temperature and more comes out once also water has sublimated. When looking at the IR spectra of these experiments, it is noticed that methane desorbs not only at its sublimation or water crystallization temperature but it is a continue and slow process. This is due to the continuous change in ASW structures during warming up (Jenniskens & Blake 1994).
2. During temperature cycles, performed back and forth from 30 K to 140 K, the desorption process of methane is slower for mixed ices, than for layered ones, thus meaning that if comets present a mixed structure, they will undergo more cycles before losing all their volatiles. During these cycles, water is observed to perform the change of phase from amorphous to crystalline and then to a better crystalline cold. By reaching only 140 K and not 200 K still some methane is retained, while water does not sublimate much.

3. The higher the thickness of a layer of crust on top of the mixture, the higher the temperature at which methane desorbs, since it is more difficult at colder temperatures, for the molecules trapped in the nucleus, to go out with a crust on top, and the more orbital cycles, in order for the lower layers to desorb. However, a larger quantity of methane is observed to go out, the thicker the layer. This is because, according to what is studied in Gundlach et al. (2011), the normalized rate of penetrating molecules through a dust layer is inversely proportional to its thickness and thus the thicker the layer the more molecules go out. After water crystallizes, the intensity with which methane goes out decreases, the thicker the crust, due to the fact that always less quantity is retained. This, however, brings to a higher desorption temperature.
4. Through this study, the desorption patter of some volatiles in comets from Biver et al. (2002), along their orbit, has been reproduced. Some of the slopes within the patterns have been linked to methane sublimation and water crystallization processes. Some differences are present within heliocentric distances but this is due to experimental conditions. Therefore, by following this procedure, and slightly changing it, the desorption patter of all volatiles in comets can be obtained.
5. A $1 \cdot 10^{-6}$ K/min ramp has been used to compute the shift in temperature for water crystallization and methane sublimation, using as a reference the experimented 1 and 5 K/min. As expected from the results of this work, the processes will both occur at lower temperatures. This gives great insight in sublimation and crystallization processes within cometary environments.

Future work will focus on considering another typical cometary volatile species and adding it to the mixture, thus reproducing even better cometary nucleus. Moreover a layer of crust will be differently made, by UV irradiation, in order to see possible variations in the desorption of methane and water.

These results show how important laboratory experiments are in order to observe differences, even if small, and the numerous variables that astrophysical situations are characterised of when such species are warmed up by nearby stars.

Acknowledgements. This work is a part of the MSc Thesis project performed by Carla Tamai at Delft University of Technology and it is therefore impossible not to thank the aforementioned University for giving the opportunity to move to Madrid and perform the experiments. Not to mention the CSIC Fisica Moleculare Institute in Madrid, who supported the entire work described here.

References

Alan May R., Scott Smith R., B. K. D. 2013a, The Journal of Chemical Physics, 138, 104501
Alan May R., Scott Smith R., B. K. D. 2013b, The Journal of Chemical Physics, 138, 104502
Ayotte, P., Smith, R. S., Stevenson, K. P., et al. 2001, Journal of Geophysical Research: Planets, 106, 33387
Biver, N., Bockelee-Morvan, D., Colom, P., et al. 1997a, Science, 275, 1915
Biver, N., Bockelée-Morvan, D., Colom, P., et al. 1997b, Earth, Moon, and Planets, 78, 5
Biver, N., Bockelée-Morvan, D., Colom, P., et al. 2002, in Cometary Science after Hale-Bopp (Springer), 5–14
Bockelée-Morvan, D., Crovisier, J., Mumma, M., & Weaver, H. 2004, Comets II, 1, 391
Brown, W. A. & Bolina, A. S. 2007, Monthly Notices of the Royal Astronomical Society, 374, 1006
Collings, M. P., Anderson, M. A., Chen, R., et al. 2004, Monthly Notices of the Royal Astronomical Society, 354, 1133
Combi, M. R., Harris, W. M., & Smyth, W. H. 2004, Comets II, 1, 523
De Pater, I. & Lissauer, J. J. 2015, Planetary sciences (Cambridge University Press)
Dohnálek, Z., Kimmel, G. A., Ayotte, P., Smith, R. S., & Kay, B. D. 2003, The Journal of chemical physics, 118, 364
Festou, M., Keller, H. U., & Weaver, H. A. 2004, Comets II (University of Arizona Press)
Gálvez, Ó., Maté, B., Herrero, V. J., & Escribano, R. 2009, The Astrophysical Journal, 703, 2101
Gundlach, B., Skorov, Y. V., & Blum, J. 2011, Icarus, 213, 710
Hansen, K. C., Altwegg, K., Berthelier, J.-J., et al. 2016, Monthly Notices of the Royal Astronomical Society, 462, S491
He, J., Emtiaz, S., & Vidali, G. 2018, The Astrophysical Journal, 863, 156
Herrero, V. J., Gálvez, Ó., Maté, B., & Escribano, R. 2010, Physical Chemistry Chemical Physics, 12, 3164
Jenniskens, P. & Blake, D. 1996, The astrophysical journal, 473, 1104
Jenniskens, P., Blake, D., Wilson, M., & Pohorille, A. 1995, The Astrophysical Journal, 455, 389
Jenniskens, P. & Blake, D. F. 1994, Science, 265, 753
Kerkhof, O., Schutte, W., & Ehrenfreund, P. 1999, Astronomy and Astrophysics, 346, 990
Kossacki, K. J. 2021, Icarus, 368, 114613
Kossacki, K. J., Leliwa-Kopystynski, J., Witek, P., Jasiak, A., & Dubiel, A. 2017, Icarus, 294, 227
Krause, M., Blum, J., Skorov, Y. V., & Trieloff, M. 2011, Icarus, 214, 286
Linstrom, P. J. & Mallard, W. G. 2001, Journal of Chemical & Engineering Data, 46, 1059
Marboeuf, U., Schmitt, B., Petit, J.-M., Mousis, O., & Fray, N. 2012, Astronomy & Astrophysics, 542, A82
Martín-Doménech, R., Caro, G. M., Bueno, J., & Goesmann, F. 2014, Astronomy & Astrophysics, 564, A8
Mastrapa, R., Sandford, S., Roush, T., Cruikshank, D., & Dalle Ore, C. 2009, The Astrophysical Journal, 701, 1347
Maté, B., Carrasco-Herrera, R., Timón, V., et al. 2021, The Astrophysical Journal, 909, 123
Maté, B., Cazaux, S., Satorre, M. Á., et al. 2020, Astronomy & Astrophysics, 643, A163
Minissale, M., Aikawa, Y., Bergin, E., et al. 2022, ACS Earth and Space Chemistry, 6, 597
Mispelaer, F., Theulé, P., Aouididi, H., et al. 2013, Astronomy & Astrophysics, 555, A13
Molpeceres, G., Satorre, M. A., Ortigoso, J., et al. 2017, Monthly Notices of the Royal Astronomical Society, 466, 1894
Pat-El, I., Laufer, D., Notesco, G., & Bar-Nun, A. 2009, Icarus, 201, 406
Rubin, M., Engrand, C., Snodgrass, C., et al. 2020, Space science reviews, 216, 1
Snodgrass, C., Opitom, C., de Val-Borro, M., et al. 2016, Monthly Notices of the Royal Astronomical Society, 462, S138
Stern, S. A., Colwell, W. B., Festou, M. C., et al. 1999, The Astronomical Journal, 118, 1120
Strazzulla, G. 1999, Composition and Origin of Cometary Materials, 269

3

Conclusions and Future Work

In this chapter the conclusions, in section 3.1, will be discussed, by answering to the research questions initially proposed and the recommendations for future work, in section 3.2, are given.

3.1. Conclusions

To better sum up the conclusions from both the small and large scale experiments described in chapter 2 and appendices, the answers to the initial research questions of section 1.1 are here reported.

1. **How does the internal morphology of cometary nuclei influence the desorption/sublimation of both volatiles and water?**

   When a temperature programmed desorption of layered or mixed water and methane ices is performed from 30 K to 200 K three desorption peaks (P_1, P_2 and P_3) occur. When the type of ice deposition changes, from layered to mixed, more methane is trapped at low temperatures and more comes out once water has sublimated. It is for this reason that in the first desorption peak of methane (P_1), methane comes out earlier in a layered structure, than in a mixed one. The opposite to what happens in P_1, happens in the third and last desorption peak (P_3). However, when looking at the IR spectra of both the cases of the experiments, it is noticed that methane desorbs not only in these three peaks but it is a continue and slow process, due to the continuous change in ASW structures during warming up.

2. **How does the heating ramp, along the orbit of a comet, influence the way in which species desorb and sublimate?**

   When the heating ramp changes, the characteristics of desorption of methane change. For a faster ramp, the desorption happens later, at higher temperatures, both for a mixed and a layered structure. This is due to the conductivity along the ice. The higher the heating ramp, the more difficult it is to have the same temperature in the sensor and in the ice, and even more difficult it is to have the same temperature along the whole ice structure, since it is not a good conductor. Moreover, the shift in temperature is larger in the case of mixed structure, rather than layered one, due to the binding energies, which are stronger in the mixed case.

3. **What is the influence of the crust on the desorption and sublimation of such species from the inside of cometary nucleus?**

   The higher the thickness of a layer of crust on top of the ices, the higher the temperature at which methane desorbs, since it is more difficult at colder temperatures to go out with a crust on top. The more the dust surrounding the nucleus of a comet and thus the thicker its layer, the more difficult it will be for molecules trapped in the nucleus to go out at relatively low temperatures. Therefore, higher temperatures are needed and thus multiple orbital cycles are needed in order for these lower layers to desorb. Nonetheless, a larger quantity of methane is observed to desorb at low temperatures, the thicker the layer. This is because, according to Gundlach et al. (2011), the

normalized (w.r.t. the gas production rate without any dust layer) rate of molecules penetrating through a dust layer is inversely proportional to its thickness and thus the thicker the layer the more molecules go out. The temperature of the dust layer remains high enough in order to not have any re-condensation of the molecules in between itself. To explain this, the resistivity model for which a dust layer is treated as a resistor to the gas flux is used. After water crystallizes, at around 140 K in the experiments, the intensity with which methane goes out is opposite to the one in P_1, thus it decreases. This is due to the fact that always less quantity is retained, even though the temperature keeps increasing, the thicker the crust.

4. **Does the desorption of methane and water change when two temperature cycles are performed?**

   The desorption process of methane is slower for mixed ices, than for layered ones, thus meaning that if comets present a mixed structure, they will undergo more cycles before losing their volatiles. During the two temperature cycles performed back and forth from 30 K to 140 K, water is observed to perform the phase changes from amorphous to crystalline and then to a better crystalline cold. In the experiment the T is increased up to 140 K and not 200 K, therefore still some methane is retained.

5. **How does the morphology of water ice change the sublimation process ?**

   It is seen how much more sublimation is generated when the particles are created with water ice grains with a higher temperature than for Liquid Nitrogen particles at a colder temperature. Between ice particles and blocks of ice it is clear that the particles lead to a bigger surface area and therefore have a major impact on the sublimation process.

6. **How does the presence of impurities (for example, titanium dioxide) influence the sublimation of water ice ?**

   When adding titanium powder to the ice, the sublimation process is way slower. Much more effect is given when liquid water and titanium are mixed and the ice is, then, raised, rather than mixing water ice and cold titanium at a later stage. The difference in the ice surface pressure is of around 0.3 mbar.

3.2. Recommendations and Future Work

As discussed in chapter 2, this study has been performed with the aim to publish a scientific paper. Therefore, the future research work that can come out from this is very wide and consists of many different options.

1. Experiments have been performed with only one layer of CH_4 and one of H_2O. To better represent the nucleus of comets, it is suggested to complicate a bit the experiments by adding more layers.

2. As a follow up from the previous point, it would be even better to add layers of also other different volatiles such as CO, CO_2, NH_3, etc. In order to do so, however, attention must be paid in the stoichiometry ratios volatile-water in comets, and try to respect them.

3. When considering the crust and thus indene, there was no opportunity to perform experiments with UV lamp in order to irradiate the gas and create a processed crust, more similar to cometary environments. It would for sure bring additional value to the research to try it out.

4. To continue with the previous point, another step would then be to change either the thicknesses of the crust to see its influence on the desorption process, or the species considered.

5. Since it might be that cometary nucleus much better behave as mixed ices inside,it is recommended to mix, according to the correct stoichiometry ratio, more and different volatiles, in such a way that it gets always more and more similar to the nucleus of comets.

6. Last but not least, temperature cycles have been performed. New ones should be done with the just mentioned variations. Moreover more than two cycles, even if with longer experimental time, might be interesting to do, to better study the evolution of cometary nuclei.

Apart from the research work dedicated to the journal, experiments have been carried out in a different laboratory in order to study the effects of lower vacuum and larger scales. However, this work could keep going forever, because many factors and variables can be changed. Some ideas for future work are here pointed out.

1. The laboratory in which the experiments have been done was lacking of a freezer/cooling system. Therefore the ice that needed to be analysed was, when ready, brought from one building, where the freezer was available, to another one where the laboratory was present. This, however, caused problems in terms of temperature and thus presence of liquid water into the container. It is thus suggested to choose carefully the methods with which create the ice and probably use cooling bags for the transport.
2. The setup at the moment the experiments have been performed was not very much equipped. Only two pressure sensors and three thermocouples were available and connected for data acquisition. Therefore it is suggested, when more of both are implemented, to record the measurements with at least 4-5 pressure sensors and thermocouples, in order to have a better idea on what happens on the ice surface.
3. All the experiments have been performed without the use of any external heat source. Therefore it is strongly suggested to use an IR lamp (and appropriate temperature regulators/controllers) to warm up the sample and thus make the sublimation process more visible.
4. Ice block or ice particles have been created. However, it might be that water ice in form of snowflakes gives better or at least more evident results.
5. The water ice was kept inside a very simple plastic container. However this brought the ice to rapidly change the temperature when put inside the vacuum chamber. A cooling plate or anything that would not influence the sublimation process (such as a glass container) might be recommended.
6. Other methods to manually check if sublimation occurred should be investigated, such as filming the entire experiment with an appropriate camera. In the present work the sample was weighted before and after the experiment, leading to many uncertainties on what sublimated (if water or titanium for example) and to which extent it is not influenced by other things, such as evaporation of the water etc.

A

Journal clarifications and extensions

A.1. Calculations regarding ”Water Ice Morphology” chapter

To support the behaviour of water ice morphology during temperature cycles, Equation A.1 and Table A.1 are used.

Equation A.1 has been taken from the gas kinetic theory from Maté et al. (2003):

$$\frac{dx}{dt} = \frac{\alpha P_{\mathrm{g}}}{\rho\,(T_{\mathrm{s}})\sqrt{2\pi m_{\mathrm{g}} k T_{\mathrm{g}}}} - \frac{v_0}{\rho\,(T_{\mathrm{s}})}\exp\left(-\frac{E_{\mathrm{d}}}{RT_{\mathrm{s}}}\right) \tag{A.1}$$

where x is the thickness of the film, α is the condensation coefficient, P_g and T_g are the pressure and temperature of the gas (water vapor) in the chamber, T_s is the substrate temperature, $\rho(T_s)$ is the ice density corresponding to this temperature, m_g is the mass of the gas molecules, k is the Boltzmann constant, v_0 is the zero-order desorption pre-exponential factor, R (or K depending on the units of E_d), in this case, is the product of the Avogadro number and the Boltzmann constant, and, finally, E_d the desorption activation energy. In this paper, the second term of the right hand side part of the equation is neglected assuming zero-order kinetics for the evaporation of the ice, and the condensation coefficient expected to be equal to 1.

The formula above is derived using the expression that describes the rate of collisions of gas molecules with a wall (effusion), that is derived from the Maxwell distribution (as in Lewis and Gladstone, 1960), and presents, on the right hand side, two terms: the first one describes the process of accretion and the second one the one of sublimation.

To estimate the number of molecules that merge, with this equation, the density can be moved to the left hand side and the following is obtained:

$$N[molec/cm^2] = x[cm] \times \rho[molec/cm^3] \tag{A.2}$$

In this way, starting from the pressure, and without the necessity to suppose any density for the ice, the number of molecules that deposit can be estimated. It thus follow table A.1 with the calculations.

	First Increase 30-140 K	First Decrease 140-30 K	Second Increase 30-140 K	Second Decrease 140-30 K
Layered, H_2O Pressure Averaged [mbar]	4.55E-08	2.80E-08	2.96E-08	2.56E-08
dN/dt [molec/(cm^3 × s)]	1.63E+17	1.01E+17	1.06E+17	0.92E+17
Mixed, H_2O Pressure Averaged [mbar]	2.65E-08	2.09E-08	2.17E-08	2.01E-08
dN/dt [molec/(cm^3 × s)]	0.95E+17	0.75E+17	0.78E+17	0.72E+17

Table A.1: Residual water pressure and water ice growth rate during the two temperature cycles for both the experiments performed on layered and mixed ices.

In the first row, the pressure, calibrated, in mbar (throughout the cycle) is reported and, whenever the growth rate was computed, the corresponding pressure, of that specific temperature cycle, was used, since the pressure was not perfectly constant throughout the entire experiment.

A.2. Application for Comets

When it comes to apply the work presented in this paper to comets, their characteristics and their orbital behaviour, different points of view can be analysed. In this case, in section A.2.1, both the crystallization temperature and the methane sublimation temperature in cometary environments are analysed. In addition to this, in section A.2.2, a comparison of the desorption pattern of volatiles in comets between the one found in literature and the one obtained in this work is done, together with a further explanation of the different slopes present in both plots.

A.2.1. Water crystallization and methane sublimation temperature in cometary environments

In chapter 2 it has been studied the temperature programmed desorption of both methane and water (layered or mixed) during two different types of heating ramp (1 and 5 K/min). However, as previously mentioned, these ramps do not really represent the one that comets undergo during their orbital cycles. Therefore, it is interesting to study how much the desorption peaks for both methane and water are shifted (in terms of temperature) when a very low heating ramp (of about 0.000001 K/min) is taken into account.

In order to graphically show this, the following procedure has been adopted:

$$T_i = T_{i-1} + \Delta T \tag{A.3}$$

$$R_i = \nu \cdot e^{-Eb/T} \tag{A.4}$$

$$N_i = N_{i-1} - N_{i-1} \cdot R_i \cdot time \tag{A.5}$$

$$TPD_i = N_{i-1} \cdot R_i \cdot time \tag{A.6}$$

where time is set in order to indicate the time it takes for the ramp to do ΔT = 0.1 K, then N is the number of molecules per square meter surface area (which is 10^{15} for water and 10^{14} for methane) multiplied by 10000 layers. The sublimation rate (R) is then given by equation A.4, with ν which is the pre-exponential factor, E_b the binding energy, and T the temperature from 30 to 180 K (as in the experiment described in chapter 2). Regarding E_b, while for water a value of 5800 K (taken from Minissale et al. (2022)) is used, for methane instead, 1650 K is considered (rather than 1232 K). This is due to the fact that it is considered the sublimation temperature of methane when covered or mixed with water, rather then the one for pure methane sublimation. Therefore, as seen in chapter 2, its sublimation temperature peak (T_{peak}) is not as usual at around 35 K but mostly at 55 K, and therefore the new binding energy, according to Luna et al. (2014), can be obtained by multiplying T_{peak} by 30.

Finally, in Figure A.1 the TPD as a function of T has been plotted.

As also seen in chapter 2, the faster the heating ramp the higher the desorption temperature. As a consequence, when considering a ramp of 0.000001 K/min, the desorption peak for both water and methane is expected, and confirmed in figures A.1a and A.1b, to be shifted to the left, at lower temperatures.

This shows that the heating ramp has a very big influence on the desorption of volatiles and therefore needs to be taken into account for further studies since these shifts allow to relate them to the temperature increase and decrease seen by comets along their orbits and are therefore of enormous astrophysical relevance. It goes without saying that these aspects do not take into account many more effects and parameters that can be found in comets, such as the fact that a non-linear heating ramp is

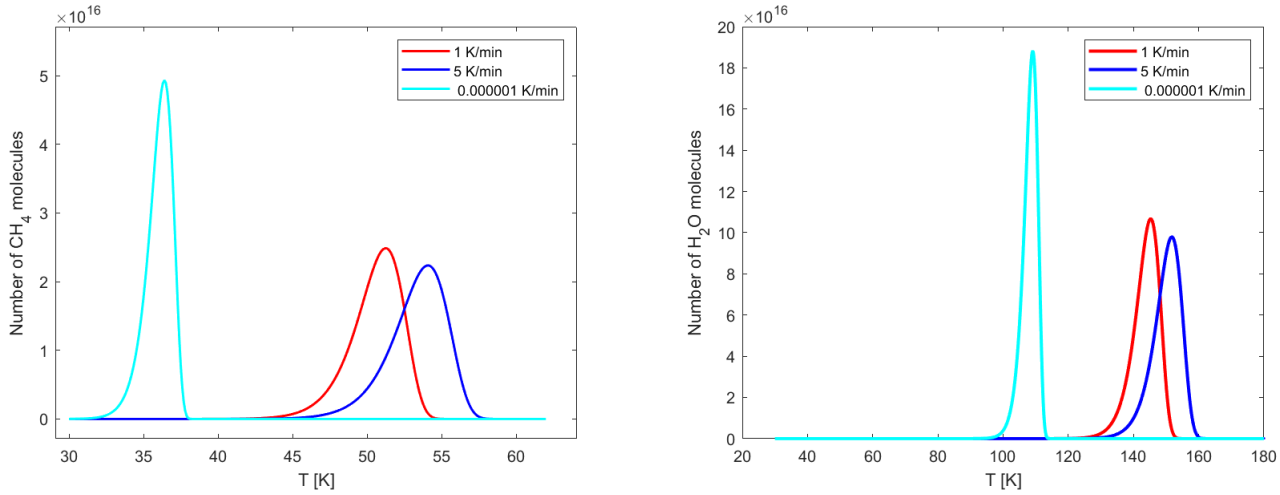

(a) TPD measurements for CH_4 molecules at different heating ramps. (b) TPD measurements for H_2O molecules at different heating ramps.

Figure A.1: TPD measurements for CH_4 and H_2O molecules at different heating ramps.

characteristics in comets, due to different velocities along the orbit, thus leading to the conclusion that some results might be approximated. However, this can be a good start to see the water crystallization and methane sublimation temperature in cometary environments.

A.2.2. Desorption patter of volatiles in comets

In Figure A.2b, the production rate, as a function of the distance to the Sun, of many volatile species in comets such as CO, HCN, CS, and OH is shown. According to this, Figure A.2a is generated to compare the results of this work with the literature, by generating the logarithmic plots of the cyan lines in figures A.1 and using equation A.7 for the equilibrium temperature of a planet, to find the heliocentric distance of the comet, starting from the temperature aforementioned:

$$T_{\mathrm{eq}} = \left(\frac{\mathcal{F}_{\odot}}{r^2_{\odot_{\mathrm{AU}}}} \frac{(1 - A_{\mathrm{b}})}{4\epsilon\sigma} \right)^{1/4} \tag{A.7}$$

where T_{eq} is the equilibrium temperature of the comet in this case, $F_{\odot}$ is the solar constant (equal to 1.37×10^3 J/(m^{2}s)), A_b the albedo of the planet/comets (supposed to be equal to 0.04 from Buratti et al. (2016)), ϵ, the emissivity, supposed to be equal to 1, σ the Stefan-Boltzmann constant, and $r_{\odot_{AU}}$ the distance between the planet/comet and the Sun, in AU.

Figure A.2a shows that the trend of the productions rate of CH_4 and H_2O very similarly reproduces, before perihelion, the one from Biver et al. (2002) of CO and OH respectively in Figure A.2b, as noticed by Collings et al. (2004).

By looking at the area of interest of this discussion, which is the left side of the blue line in Figure A.2b, two different slopes for both OH and CO can be noticed. More precisely, the slopes change around 3 AU for both molecules. This can be related to the release of methane and the crystallization of water. As studied in Marboeuf et al. (2012), it is the structure of water ice that influences the outgassing process of the other volatiles. What changes during a TPD, is indeed the temperature at which methane starts desorbing. In Figure A.2b it can be seen how, little after 2 AU from the Sun, a peak in the production rate of volatiles is seen. This might indeed be related to their desorption when the crystallization of water ice starts.

The only difference that is noticed is, in Figure A.2a, within the astronomical units at which the desorption processes are happening, with respect to what is seen in Figure A.2b. However, this is only a problem of the quantity of methane and water present in the experiment/calculation, and due to the

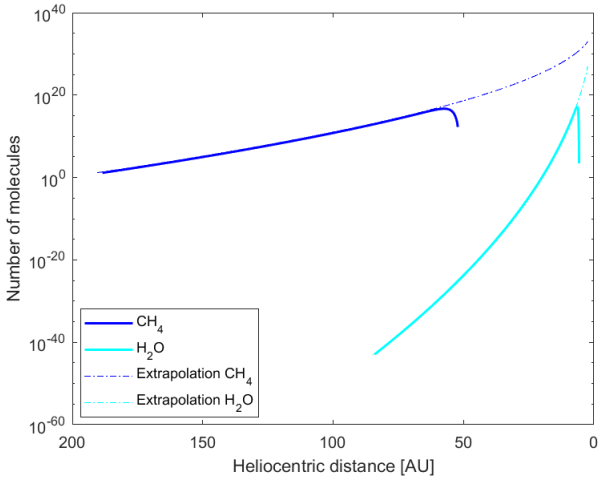

(a) Production rate (in logarithmic scale) for water and methane molecules as a function of the heliocentric distance, together with extrapolation of their trend.

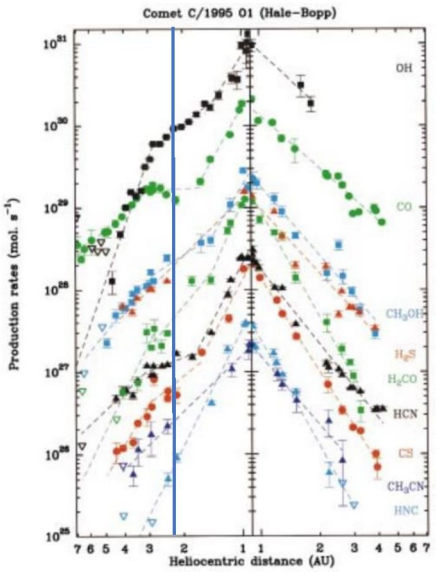

(b) Production rate of different species in Comet Hale-Bopp. Image retrieved by Biver et al. (2002), and modified by Carla Tamai for thesis project explanation purposes.

Figure A.2: Comparison between literature and thesis work regarding desorption patter of CH_4 and H_2O during cometary evolution along the orbit.

fact that in this work internal layers are considered during temperature cycles, rather than the surface of the comet, which is instead considered in the literature. Therefore, the peak, in our case is shifted a bit more to the left, further away from the Sun, because of the lower temperatures that reach the more internal layers. To better present the work from Biver et al. (2002), an extrapolation has been computed in order to be able to see the behaviour of these two molecules when close to the Sun, in between 7 and 0 AU.

By following this work, very important considerations can be made on the behaviour of many different species in the nucleus of comets, extending the computation to temperature cycles, and considering larger layers of such species.

B

Additional experiments from phase 1 in Madrid

During the period in Madrid, other experiments were performed but, since the results obtained would have needed much more time to be analysed than the one available, they were not included in the paper reported in this project. In addition to this, some of the experiments would have broaden the main topic too much, thus distracting and confusing the reader. However, it is supposed that these results are promising and can lead to important studies. Therefore, they are here reported, with just suggested ideas on how to interpret them and proceed with them in the future.

Before removing the radiation shield, which is inside the vacuum chamber aforementioned, the following experiments were performed as a first try:

1. Layered structure, 5 % stoichiometry ratio, 5 K/min
2. Layered structure, 1 % stoichiometry ratio, 5 K/min
3. Mixed structure, 1 % stoichiometry ratio, 5 K/min

They are reported in Figure B.1a and B.1b for, respectively, methane and water.

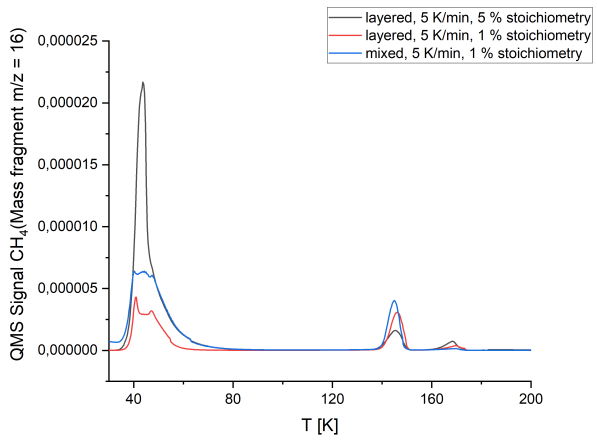

(a) Comparison of QMS signal for CH_4, as a function of temperature, in layered and mixed experiments (with H_2O) with radiation shields in the vacuum chamber.

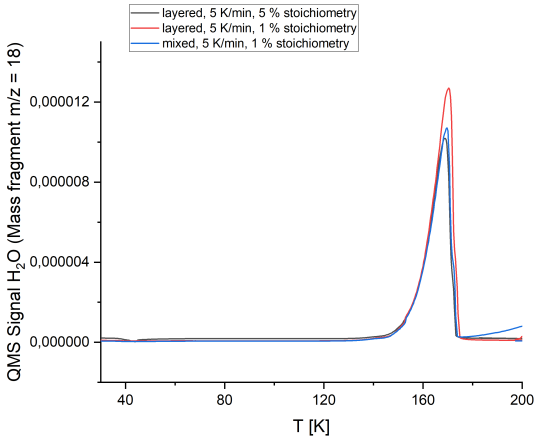

(b) Comparison of QMS signal for H_2O, as a function of temperature, in layered and mixed experiments (with H_2O) with radiation shields in the vacuum chamber.

Figure B.1: QMS signal for CH_4 and H_2O with effect of radiation shield within the chamber.

As it can be noticed in Figure B.1a, at around 140 K, differently from what shown in the experiments reported in the paper, there is only one peak and not two. This can be due to the presence, in this case, of the radiation shield inside the vacuum chamber.

Apart from this difference, since the ramp used is always the same, no shifts in the peaks can be observed. Only a difference in the intensity of the desorptions is noticed due to a difference in the stoichiometry ratio adopted. The well known and already mentioned diversities between a mixed and a layered structure, instead, are detectable.

Different stoichiometry ratios (between water and methane) have been changed in order to see what the effects would have been on the desorption of methane through ASW ice, therefore the following experiments were done:

1. Layered structure, 5 K/min, 3 % stoichiometry ratio
2. Layered structure, 5 K/min, 2 % stoichiometry ratio
3. Layered structure, 5 K/min, 1 % stoichiometry ratio

They are shown in Figure B.2a and B.2b.

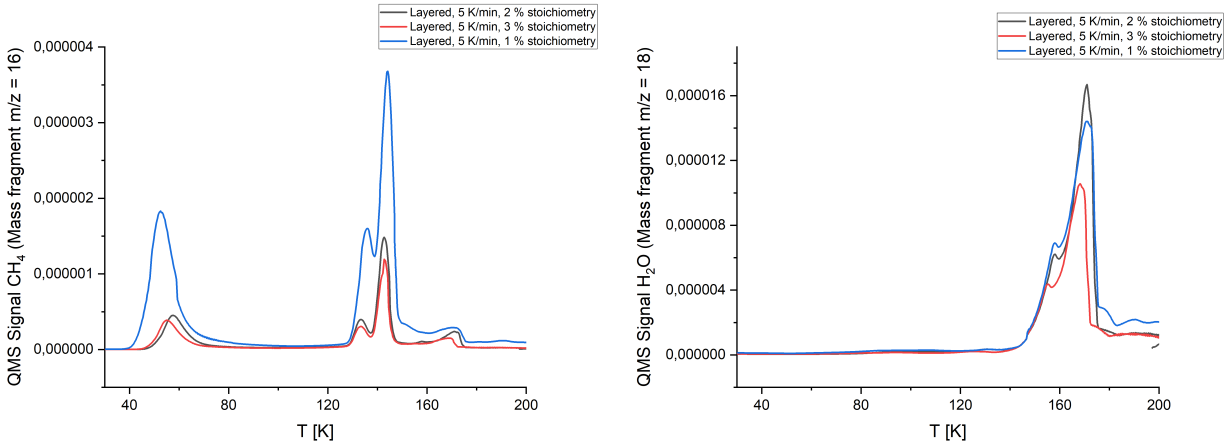

(a) QMS signal for CH_4 as a function of temperature, for different stechiometry ratios between methane and water, for a layered structure and a 5 K/min heating ramp.

(b) QMS signal for H_2O as a function of temperature, for different stechiometry ratios between methane and water, for a layered structure and a 5 K/min heating ramp.

Figure B.2: QMS signal for CH_4 and H_2O for different stoichiometry ratios.

These figures, however, show some problems due to the absence of the radiation shield in the QMS signal, which cannot be reliable to give explanations on the behaviour of the experiments. While it can be seen that there is no shift in temperature, since the heating ramp is not changed, it still can be seen a difference in the intensity of the QMS Signal, due to the difference in the stoichiometry ratio.

On the other hand, for water there is not very much to say because, as already known, since the heating ramp is always the same, no shifts in the peak can be noticed, and only the intensity of the desorption changes, in such a way that the more water is in the mixture, the more it desorbs.

Just to conclude this part, since in the paper only graphs with normalised QMS are reported, here the normal ones are shown in Figure B.3, B.4a and B.4b, so that comments can be done also on the second peak of desorption of methane.

In Figure B.4b, at a temperature of about 135 K, the second peak results to be bigger in intensity for the quicker ramp (5 rather than 1 K/min), and a shift in temperature is present, with a higher temperature for the quicker ramp peak. The latter is already explained in the paper but regarding the intensity, the reason can be due to the amount of gases and molecules initially put in the chamber. The ratio is still more or less the same, but that does not imply that the quantities are also equal. The same can be said for Figure B.4a. In Figure B.3 it is to notice that the ramp is the same and thus no shift in the

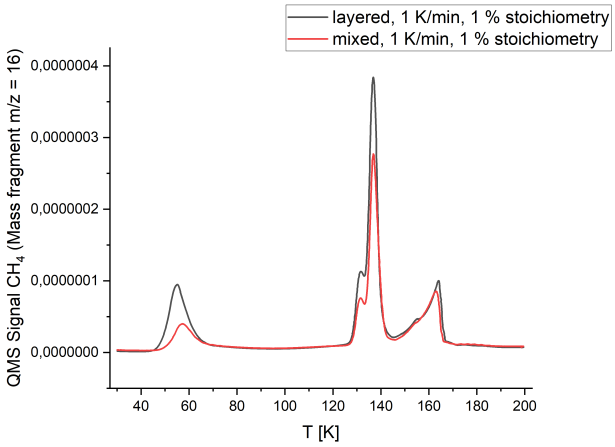

Figure B.3: QMS signal for CH_4 with respect to temperature, for both a layered and a mixed structure (together with H_2O, in a stoichiometry ratio of around 1 %) and two different heating ramps, 5 and 1 K/min.

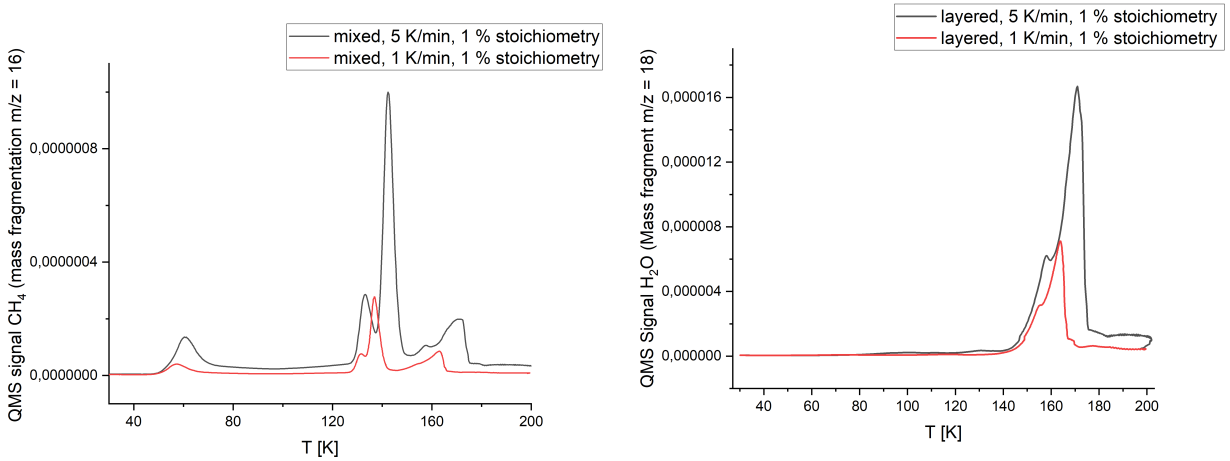

(a) QMS signal for CH_4 with respect to temperature, for a mixed structure (together with H_2O, in a stoichiometry ratio of around 1.2%) and two different heating ramps, 5 and 1 K/min.

(b) QMS signal for H_2O with respect to temperature, for a layered structure (together with CH_4, in a stoichiometry ratio of around 1 %) and two different heating ramps, 5 and 1 K/min.

Figure B.4: QMS signal, not normalized, of methane and water, for different experiments.

temperature of the peak is present. However, just a change in the intensity of the peak is seen. This is because for a layered structure, when water sublimates, it is easier for methane to desorb, as already mentioned in the paper, due to the presence of pores and voids in which to go through.

About the experiments on temperature cycles, there is one thing that was not mentioned in the paper which is a peak, in the QMS signal versus temperature plots, that happens right at 30 K, for methane, when the second cycle begins and that is supposed to be the multi-layer effect.

When cooling down water tends to remove methane thus leading the latter to segregate. However, there are parts in which methane is still mixed with water and others in which it is in a layered configuration. For this last case, methane is almost all desorbed in the first heating ramp, due to the fact that the binding energy between methane and methane is weaker than between methane and water. On the other hand, for the mixed parts, during the cooling when water molecules reorganize themselves, methane creates multi-layers and when the heating ramp is started, it immediately desorbs from this layers.

This effect can be seen in Figure B.5a and B.5b.

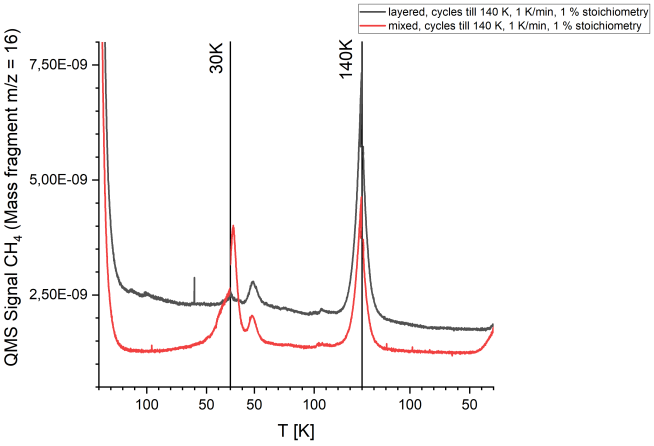

(a) QMS results of desorption of methane through ASW ice during the first cooling down and the second entire temperature cycle from 30 to 140 K.

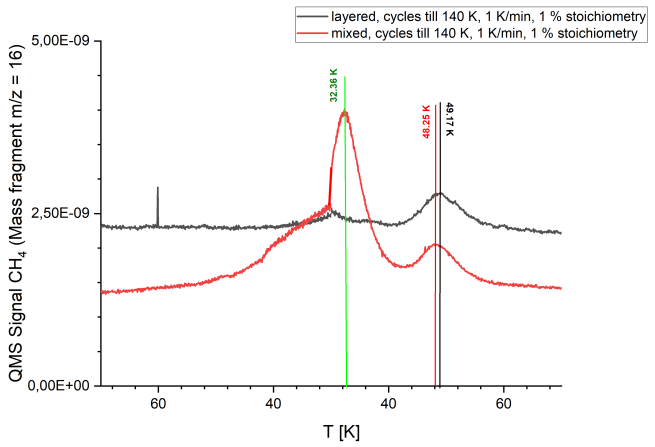

(b) Zoom on the QMS results of desorption of methane through ASW ice during the second warming cycle, at 30 K.

Figure B.5: Desorption of methane through ASW ice during temperature cycles.

When the experiments with the crust were performed, very useful information were obtained studying the behaviour of indene. A phase transition, in the plot integral versus temperature, can be seen at around 125-130 K. Figure B.6a explains the strange decrease of observed indene in Figure B.6b.

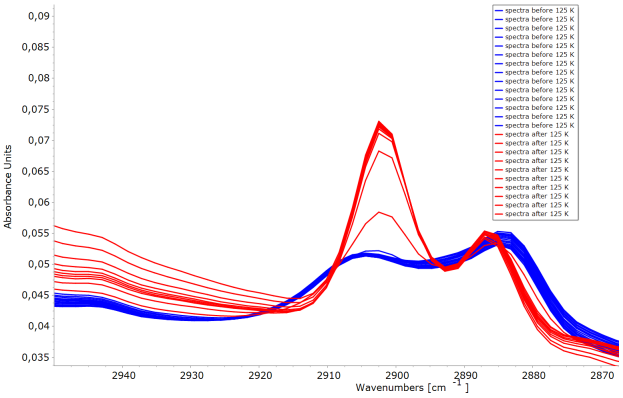

(a) IR spectra of indene at wavenumber around 2900 cm^{-1}.

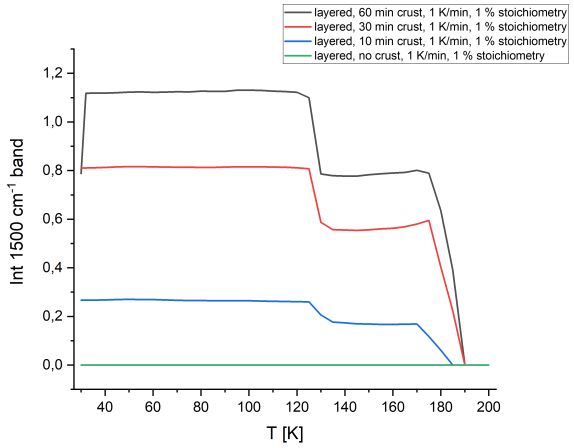

(b) Integral of the band of indene, through all the experiment band spectra at around 2900 cm^{-1}.

Figure B.6: Phase transformation of indene

Even in this case, the graph without normalised results is reported in Figure B.7.

As previously said, the second peak is the only thing to look at in this case and it seems, due to the explanation given in the paper, the thicker the crust, the more methane desorbs.

Last but not least, when the crust is added it has not been well shown, in the paper, how water behaves. Therefore Figures B.8a and B.8b are reported.

The first very interesting thing that can be proved with these images is that at the end of the experiment the water is all gone, even though a layer of crust is present on top of it. In Figure B.8a it is also seen the effect of the crust on the sublimation temperature of water. The thicker the layer the later the sublimation. Moreover, less water seems to come out, the thicker the layer of indene, but this is due

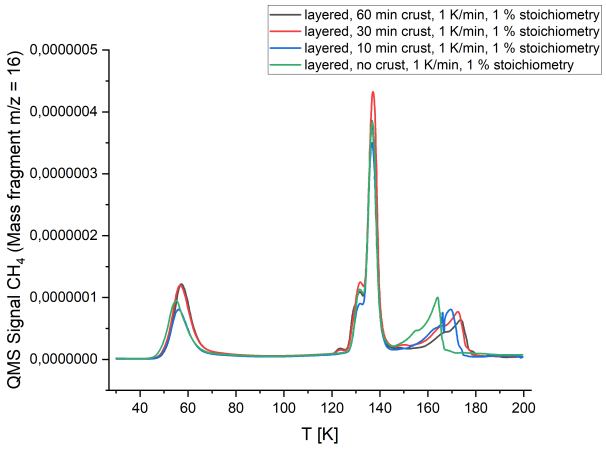

Figure B.7: QMS signal of methane desorption through ASW ice, with respect to temperature, for different experiments with a different thickness of the crust of indene.

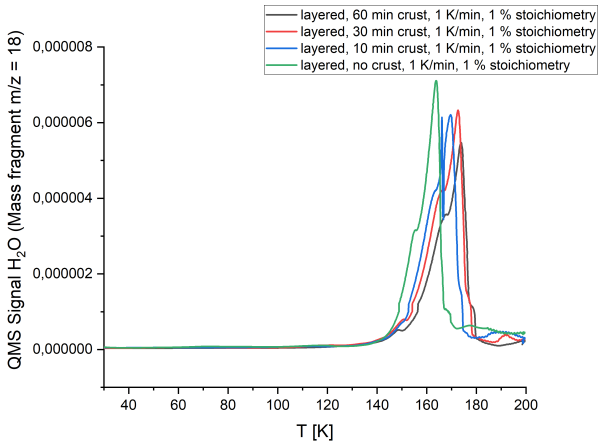

(a) QMS signal of water, with respect to temperature, for different experiments with a different thickness of the crust of indene.

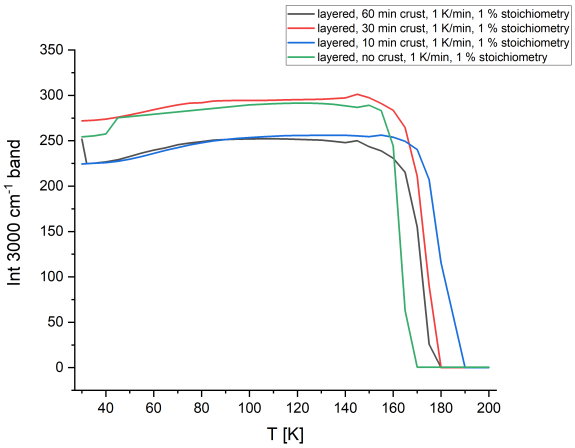

(b) IR spectra of water at wavenumber around 3000 cm^{-1}.

Figure B.8: QMS signal and IR water results during desorption when a layer of crust of indene is on top of it.

to the fact that, looking at the stoichiometry ratio (from 1.2 to 1.29 %), a smaller quantity of water is present. In Figure B.8b the behaviour of water, analysed in the paper, can be used as an additional confirmation.

C

Main experiments in Delft: phase 2

In order to do a comparison between small and large scale experiments, the laboratory of the wind tunnel at the University of Technology of Delft has been used.

C.1. Experimental setup and procedure

In this chapter, the experimental setup and procedure taken into account for the tests is described. In section C.1.1 the entire set up and equipment is revised and in Section C.1.2 the procedure adopted for every experiment is analysed.

C.1.1. Setup

The main equipment used to perform the experiment is a vacuum chamber. The one used, however, is a section of the Hypersonic Tunnel Facility Delft (HTFD) (see Figure C.1). The latter is usually a wind tunnel that uses the Ludwieg tube wind tunnel concept Schrijer and Bannink (2010) and can generate gas flows with both a Mach number up to 11 and a Reynolds number of 8×10^6.

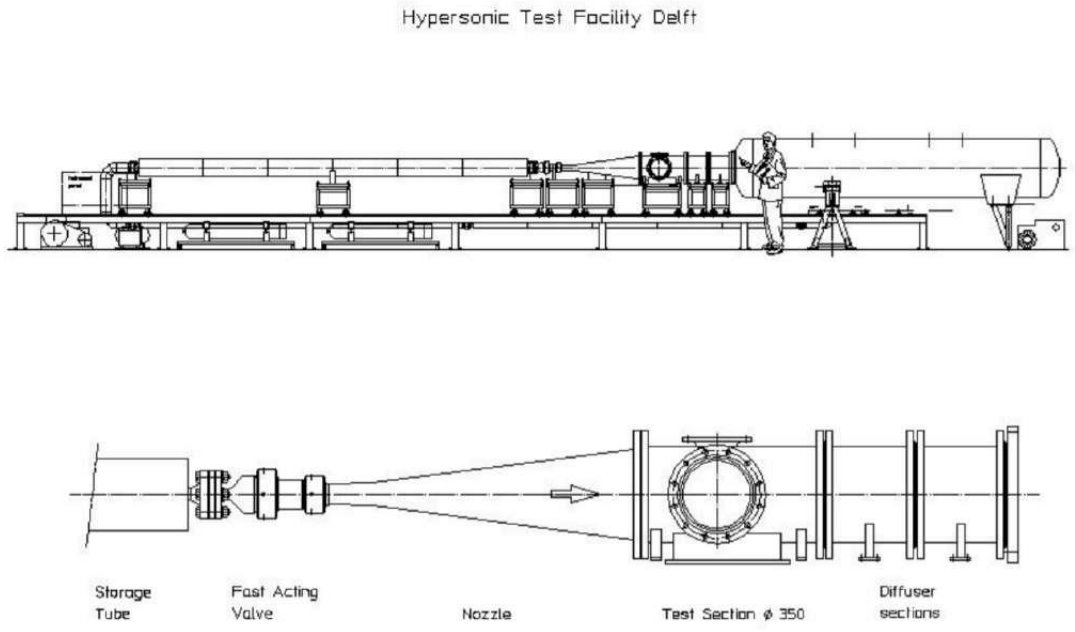

Figure C.1: Schematic of the Hypersonic Tunnel Facility Delft (HTFD) retrieved from David et al. (2006).

It is composed (from left to right) of a storage tube where a fluid can be pressurized at a controlled

temperature. Then, typical for a wind tunnel facility, there is the conical nozzle that accelerates the flowing gas to hypersonic conditions. The test section, at the exit of the nozzle, is where the flow reached the aimed conditions and therefore the site where the sample is positioned in order to study its performance at those conditions. At the exit of this test section there is a vacuum discharge tank, characterised by two vacuum pumps that helps to recreate large pressure ratios across the nozzle. In this study, only the second half of the facility is used, recreating a plain vacuum chamber with only the test section and the discharge tank. The test section has length of 350 mm, width of 200 mm and height of 640 mm. At the bottom of the test section, however, an extension has been added so that the volume and the height are increased, in case they are needed. The interior of the chamber can be accessed through a circular side-window of a diameter of 260 mm that can open when no vacuum is created in the chamber, and that can allow visual representation of the sample during experiments. This chamber is evacuated by the use of one or both the pumps and is able to reach a minimum pressure of around 0.8 mbar.

The sample is put in a cylindrical plastic container (see Figure C.2a), open on top, with a diameter of 14 cm. On the side of this container, two holes are made in such a way that pressure sensors and thermocouples can be inserted and take the measurements with respect to the distance from the surface of the ice. In some cases, a tape was put on the top of the container (see Figures C.2a and C.2b), in order to recreate a partly closed area inside the chamber and thus better notice the difference in pressure and temperature between the inside of the container and the outside. In most of the cases, though, the container was left open on the top, as seen in Figures C.3a and C.3b.

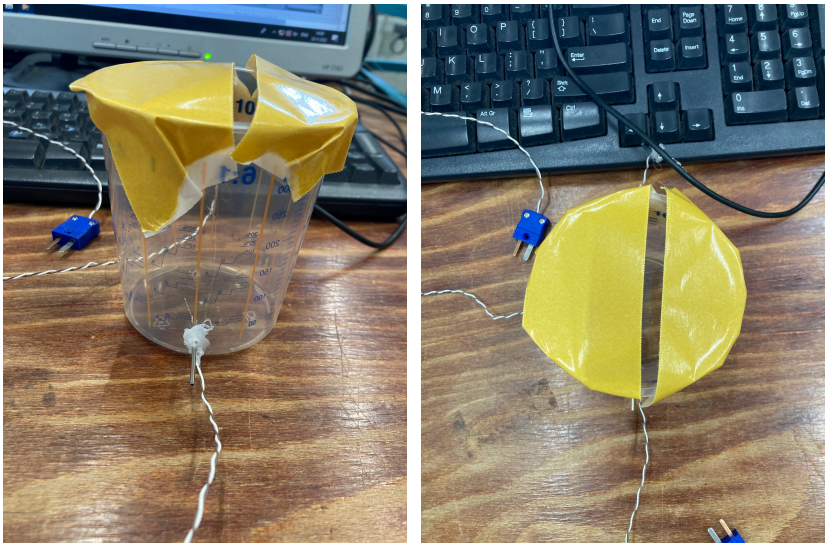

(a) Side view of the plastic container, covered on top with some tape

(b) Top view of the plastic container, covered on top with some tape

Figure C.2: (Closed) Plastic container for the experimental sample.

As briefly mentioned, the thermodynamic conditions of the sample are monitored by three T-type thermocouples, to measure the temperature, and two pressure sensors, the THERMOVAC TR 211 by Leybold and the HCLA12X5EU by First Sensor, to measure the pressure (Sklavenitis, 2022). These sensors are connected with wires to two data acquisition modules (CompactDAQ modules by National Instruments with relevant documentation in Sklavenitis (2022)). The wires pass through holes on the wall of the vacuum chamber that have been afterwards airtightly sealed. The modules are connected to a computer, and the data is acquired and logged through a LabVIEW program. Apart from sensors monitoring the local conditions (temperature and pressure), the sample is also monitored visually through the windows of the vacuum chamber.

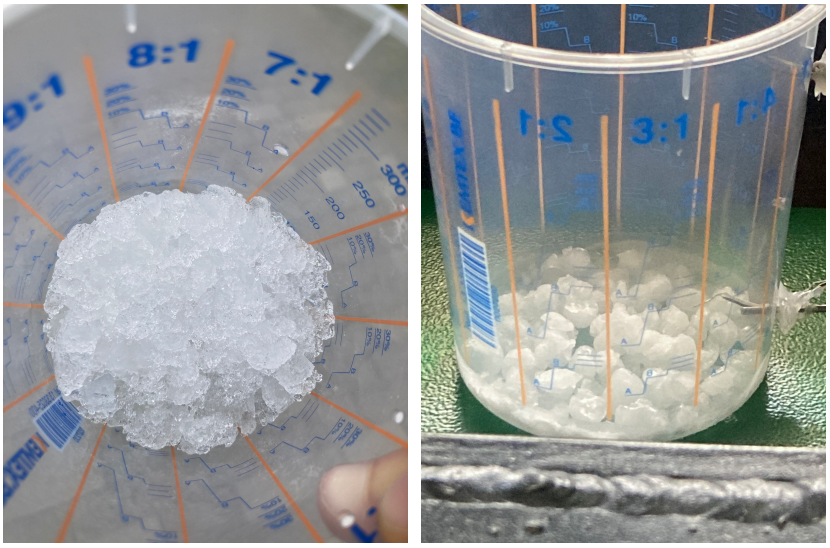

(a) Water ice grains inside the plastic container.

(b) Liquid nitrogen ice particles inside the container.

Figure C.3: Plastic container for the experimental sample with ice grains

C.1.2. Procedure

It has been seen that when doing small scale experiments there are some factors that can influence the diffusion and sublimation of some species. Therefore, it is interesting to see if the same happens when a larger scale is taken into account for the tests. Differently from Madrid, where experiments have been performed with CH_4 and H_2O and C_9H_8, in Delft mainly H_2O will be considered, since it is not possible to use other volatiles. However, some experiments do take into account titanium, TiO_2, in order to recreate the same idea of the crust that was adopted in Madrid.

Sample Preparation

Depending on the case, (distilled) water has been raised either in a freezer at around -20 °C or with liquid nitrogen, at around -200 °C. This, moreover, gives the possibility to do comparisons with the small scale experiments with regards to the temperature at which ices are risen and thus the difference in the influence of this factor on sublimation and diffusion of such species. When a block of water ice was needed, distilled water ice was used as it grew in the freezer, directly in the container. On the other hand, when ice grains were necessary, the particles where either directly taken from a specific freezer that kept the grains format or created by spraying distilled water in gaseous liquid nitrogen. Titanium, instead, has been used in a solid (powder) state.

Therefore, when the water ice is ready, the sample (the container, with water and, at a later stage, titanium too, inside) is positioned inside the vacuum chamber. Two thermocouples and two pressure sensors are inserted in the holes of the plastic container, in such a way that the lower hole is directly on the surface of the ice thus measuring the pressure and the temperature at that height, and the higher hole is right on the surface of the container thus giving insight on the gradient with which these two parameters vary. Once the chamber is closed, the pumps are activated and vacuum is created in the chamber. This low pressure eventually brings water and titanium to sublimate. When sublimation is thought to be finished, and the measurements are recorded, the experiment is finished and the pumps can be turned off. The chamber goes back to atmospheric pressure and can be open again.

C.2. Experiments

In this chapter the three set of experiments are described in Sections C.2.1, C.2.2, C.2.3. Together with them, surface areas are computed. The results and the discussions follow in the next chapter.

The general idea to start with, for the experiments in Delft is to first study the simple sublimation of

either a block or small grains of water ice. Since the minimum pressure that can be reached by the vacuum chamber is still quite high, it is good to first make sure that any kind of water sublimation is measured and noticed within the vacuum chamber. This leads to the conclusion that first a test with an empty vacuum chamber (with inside the empty container) is performed so to refer to this pressure as the minimum reachable without the influence of any species and any sublimation. Once it is made sure that sublimation of water is seen, different types of water ices are studied, followed by the addition of titanium powder either in between the grains or on top of the ice or within the ice block. In this way, these experiments allow to both study the sublimation of ASW ice, raised in different ways, by looking at a change in the pressure within the vacuum chamber and the effect that species such as titanium dioxide can have on it, simulating the crust and impurities present in the nucleus of a comet.

C.2.1. First Set of Experiments

The first set of experiments is mainly focused on water ice and its sublimation. The list of experiments performed, in order, is the following.

1. Empty chamber test to see the reachable pressure without nothing inside. The pressure results to be around 0.8 mbar
2. Big block of water ice (that broke), open container
3. Smaller block of water ice, open container
4. Water Ice grains, open container
5. Fewer water ice grains, weighted (initial weight 30 g, final weight 24 g), open container
6. Same as previous one but with the top almost fully covered with some tape (initial weight 24 g, final weight 20 g)
7. 6 g (initial weight) water ice grains, open container, 4 g final weight
8. Liquid nitrogen water ice particles, open container
9. Liquid nitrogen bigger pieces, open container
10. Liquid nitrogen ice blocks and particles, covered at the top, filmed, initial weight: 41 g, final weight: 38 g

These first experiments were mainly done to try different things and see which one would have then given interesting results. Different papers such as the ones from Jambon-Puillet et al. (2018), Moores et al. (2006), and Kaufmann et al. (2009) were analysed for suggestions on how to study sublimation of water in low vacuum conditions. From these, indeed, the idea of small particles/grains was adopted.

C.2.2. Second Set of Experiments

Once the first set of experiments was finished, results were analyzed and therefore new experiments planned. Some of them needed to be retaken, with some more precision in terms of quantity of ice to use, duration of the experiment and position of pressure sensors. Others were indeed added and others deleted. Regarding the latter, for example, it was realised that it was not very feasible to make a water ice block using the technique with liquid nitrogen and therefore that experiment was not considered anymore. In order to see if any sublimation was happening, the initial and final weight were considered, apart from a hypothetical increase in the pressure of the vacuum chamber.

The experiments in this case are:

1. Empty vacuum chamber
2. Covered container in vacuum chamber
3. Block of normal water ice, 20 g, 90 min, open container, final weight = 12 g
4. Normal water ice grains, 20 g, open container, 90 min, final weight = 13 g
5. Liquid nitrogen particles, 20 g, open container, 90 min, final weight = 16/17 g
6. Liquid nitrogen particles, 20 g, closed container, 90 min, final weight = 15 g

In order to properly compare the results and have an idea on how much water is sublimating, the surface area for each case is computed. When considering the experiments with either water ice grains or water ice particles made with liquid nitrogen equation C.1 is adopted:

$$A_s = 4\pi r^2 \cdot 20 \cdot \frac{1}{2} \tag{C.1}$$

considering the surface area of a sphere being equal to $4\pi r^2$. The latter was multiplied by 20 because, since each particle weighted more or less 1 g and the total amount of ice considered is 20 g, the surface area of a single sphere had to be multiplied by the number of all the spheres/particles. This was then divided by two since only half of the particles is facing the outside, while the other one is facing the bottom of the container and does not influence the sublimation process. Being the radius of the particles equal to 2 cm more or less, the surface area in these cases is equal to 502,7 cm^2.

On the other hand, when a block of ice is considered, the surface area of a circle can be computed. The formula to use is indicated in C.2

$$A_s = \pi r^2 \tag{C.2}$$

Since the container has a radius of 7 cm, the surface area, in this case, is 154 cm^2.

C.2.3. Third set of experiments

At this point, sublimation of ASW ice is studied and it becomes interesting to analyze the effect that a powder such as TiO_2 has on it. Therefore the experiments performed are:

1. Mix of titanium and liquid nitrogen water ice particles, initial weight = 20 g (3 g of titanium and 17 g of water), open container, 90 min, final weight = 15 g
2. Mix of titanium and water ice grains, initial weight = 21 g (20 g water, 1 g titanium), open container, 90 min, final weight = 15 g
3. Block of ice and on top cold titanium, 90 min, open container, initial weight = 20 g water + 1 g titanium, final weight = 15 g
4. Block of ice with water and titanium mixed at ambient temperature and raised together in the freezer, 90 min, open container, initial weight = 20 g water 1 + g titanium, final weight = 15 g
5. Again water ice grains and cold titanium mixed as previous one (but now colder titanium powder from the freezer), initial weight = 20 g water + 1 g titanium, open container, 90 min, final weight = 16 g

In the first experiment too much titanium was used and it was noticed that not only this did not bring to any interesting result but also it warmed the water ice in such a way that its temperature was quite high (around 10 °C).

From previous calculations it is quite straightforward to compute the surface area when the quantity of water is changed, thanks to the assumption that each water ice grain/particle weights 1 g. Therefore, in the case in which 17 g of water are used, the new surface area would be 427.295 cm^2.

C.3. Results and Discussion

In this section the final results and a small discussion about the aforementioned experiments are reported. Mainly the pressure and the temperature on top of the ice surface will be shown, as a function of time. It would have been interesting to show the pressure in the chamber and thus analyze the difference between that pressure and the one in the container but it was noticed that almost no difference was in between the two, leading to the idea that the process is that quick that immediately all the vacuum chamber sees the sublimation and the pressure is thus higher for both the chamber and the ice surface.

Figure C.4 show the pressure and the temperature, during the entire period of the experiments, on top of the ice surface, for all the different types of experiments performed. In dots there is the pressure referred to the case of the empty chamber, to use as a reference for the other tests. The temperatures remain more or less constant throughout the entire experiments, since no additional and external heating source is adopted. To better analyze these figures, ratios between the sublimation rates of every case are computed, in such a way that, by taking as a reference one case, all the others are compared.

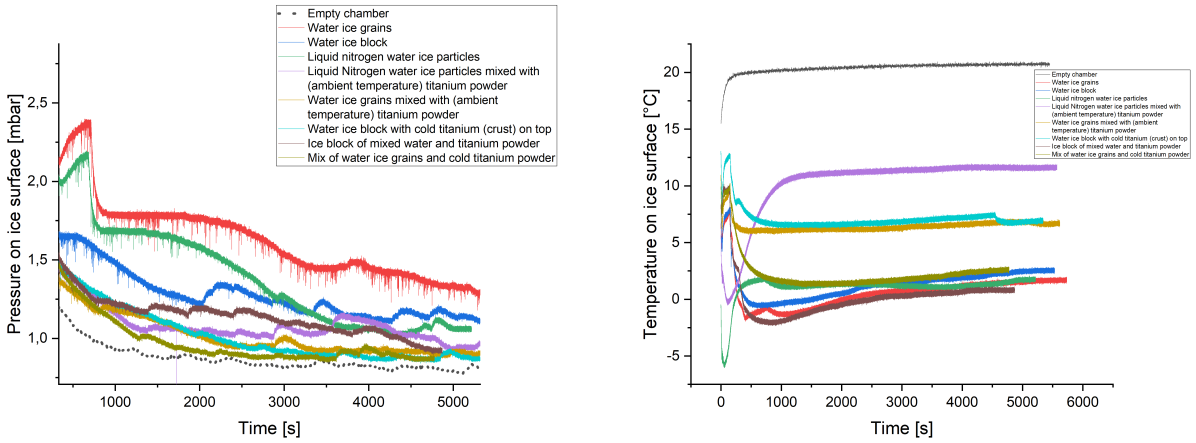

(a) Pressure on ice surface during the entire duration of the experiments.

(b) Temperature on ice surface during the entire duration of the experiments.

Figure C.4: Pressure and Temperature results from the experiments.

The ratios are computed in equation C.3, making use of the Arrhenius formula, from Minissale et al. (2022), that is an equation that describes the evaporation rate of the surface of a material giving the collision rate of molecules depending on their temperature:

$$\frac{N_2}{N_1} = \frac{A_1 \times \nu \times e^{-\frac{E_b}{kT_1}}}{A_2 \times \nu \times e^{-\frac{E_b}{kT_2}}} \tag{C.3}$$

and then checking whether it is the same as the experimental result, as in equation C.4:

$$\frac{N_2}{N_1} = \frac{P_2}{P_1} \tag{C.4}$$

where T_1 and T_2 are the temperature, in K, of the two cases on the ice surface seen from Figure C.4b (when the values get to be stable), ν is the pre-exponential factor (vibrational frequency of a given species), E_b the binding energy (activation energy for the molecules, that depends on the material/molecules), A_1 and A_2 the surface area as explained in equations C.1 and C.2, and k the Boltzmann constant. However, it is important to specify that next to the surface area there should have been the number of water molecules per square meter surface area (around 10^{20}, from Breithaupt (2000)), which, however, would have been the same for both cases on the numerator and denominator and thus is not included. When doing the actual calculation, also the pre-exponential factor is not considered, since the only thing that changes within the formula is the temperature. Water desorption rate is considered and thus the pre-exponential factor and the binding energy (respectively equal to 4.96 $\times 10^{15}$ s^{-1} and 5705 K, from Minissale et al. (2022)) are the same in both cases.

The case that is being used as a comparison for all the others is the one that considers the sample with water ice grains (red one in Figure C.4a). The results are shown in Table C.1 (explained in legend C.2), from which a comparison can be made between $\frac{N_2}{N_1}$ and $\frac{P_2}{P_1}$.

Experiment without titanium | Experiment with warm titanium | Experiment with cold titanium

	Water ice block	Liquid Nitrogen water ice particles	Liquid Nitrogen water ice particles mixed with warm titanium	Water ice grains mixed with warm titanium	Water ice block with cold titanium crust on top	Ice block of liquid water and titanium mixed	Mix of water ice grains and cold titanium
$\frac{N_2}{N_1}$	0.33	1.07	2.2	1.5	0.47	0.28	1.1
$\frac{P_2}{P_1}$	0.92	0.85	0.77	0.74	0.69	0.74	0.69

Table C.1: Ratios of sublimation rates of different cases with respect to the sublimation rate of water ice grains' case.

Color	Meaning
Blue	Ice block experiment
Cyan	Ice particles experiment

Table C.2: Legend for Table C.1.

To read Table C.1, it is important to notice that the ratios are, as aforementioned, with respect to the sublimation rate for water ice grains, which are the ones sublimating more. Therefore, the bigger the ratio, the more water is sublimating. According to this, it can be noticed that the water ice block is the one that always gives values smaller than one and this makes sense since the surface area, that is the area contributing to the sublimation process, is way smaller for the block of ice than the one for the ice particles. Successively, experiments with titanium and ice particles seems to give birth to a major sublimation, however this is probably only due to the titanium impurities, which, due to the pressure over them in the chamber, exit the container and dirty the chamber. However, the lower the temperature of the titanium powder, the less sublimation is seen, confirming the phenomena just explained, due to the fact that with a lower temperature it is more difficult for both water and the powder to sublimate. Last but not least, in the second column of table C.1 it can be seen that there is not that much difference between the sublimation of water ice grains and liquid nitrogen particles ($\frac{N_2}{N_1}$ around 1). This is because, according to Figure C.4b, the temperature is almost the same, due to the fact that even though the liquid nitrogen particles should be colder, they warm up as soon as they are inside the plastic container.

It has to be specified that while the calculations of $\frac{N_2}{N_1}$ have been done using the binding energy of water and the stable temperature value seen from Figure C.4b, the ratio $\frac{P_2}{P_1}$ from the experiments show the pressure on the ice surface which can be, however, influenced by the titanium powder. Therefore, in Table C.1 a quite big difference between the experiments and the calculations can be noticed. One interesting point is that all calculations for water ice particles are above 1 while the experimental results ($\frac{P_2}{P_1}$) are below 1. This means that a bigger surface area is needed in order to reproduce them. The opposite, instead, can be said for the water ice block experiments.

With these experiments, therefore, both the crust of the cometary nucleus and the type of deposition of the ices have been analyzed and comparisons can be made with the experiments in Madrid. When the crust is present, it is confirmed, even by these results, that less water sublimates. When it was studied the behaviour of methane and water in small scale, it was seen that the additional presence of indene on top was delaying the desorption of methane and the sublimation of water. The same thing is noticed here. During the same amount of time, way less water sublimates when titanium is present. When the ice morphology changes, differences from the results in Madrid are present. There, the mixed case was bringing to less quantity to sublimate, as seen in Appendix B. However here the presence of methane was influencing the results. Therefore, this case cannot be compared with the simple difference between ice block and ice particles experiments, performed in Delft. However, when titanium powder is added, this can be applied and the effects can be confirmed by looking at the last three columns in table C.1.

At this stage, however, it is a bit difficult to relate these results to the behaviour of comets and their molecules. Additional and further analysis would be needed in order to go more in depth with the research study.

D

Additional results from experiments in Delft

Before getting to the final results in Delft many sets of experiments have been performed in order to make sure that sublimation of water was seen in the chamber at low vacuum conditions, and then to try out different ice morphology to see which one was the one giving more sublimation.

Figure D.1 shows the first set of experiments, where different ice conditions and structures were tried. Pressure and temperature on top of the ice surface are given with respect to the duration of the experiment. All experiments have been combined in one plot since in this way it would have been easier to analyse the results. It is indeed true that in this way the difference in pressure is quite noticeable. Therefore sublimation of water is detected and quite some effects are given by the difference in the ice structure and growth temperature.

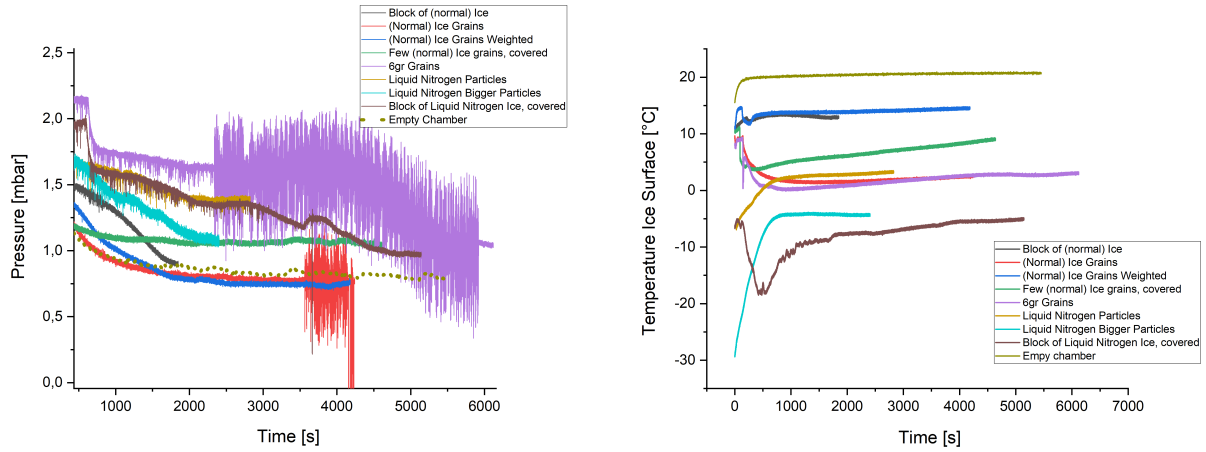

(a) Pressure on ice surface during the entire duration of the experiments.

(b) Temperature on ice surface during the entire duration of the experiments.

Figure D.1: Pressure and Temperature during the first set of experiments

For the red and purple line, in the same figure, some noise is presented at the end of the plot. It is therefore important not to consider those parts for further analysis.

In Figure D.2, the second set of experiments is presented. With this graphic it is confirmed that sublimation of water is happening and that it behaves differently depending on the morphology of the water ice and the temperature at which it is risen. More precisely, the block of water ice is the one that sublimates less, due to his smaller surface area, followed by liquid nitrogen particles, for the temperature

at which they found themselves, and then water ice grains which are the ones that sublimates more, thanks to their surface area and temperature.

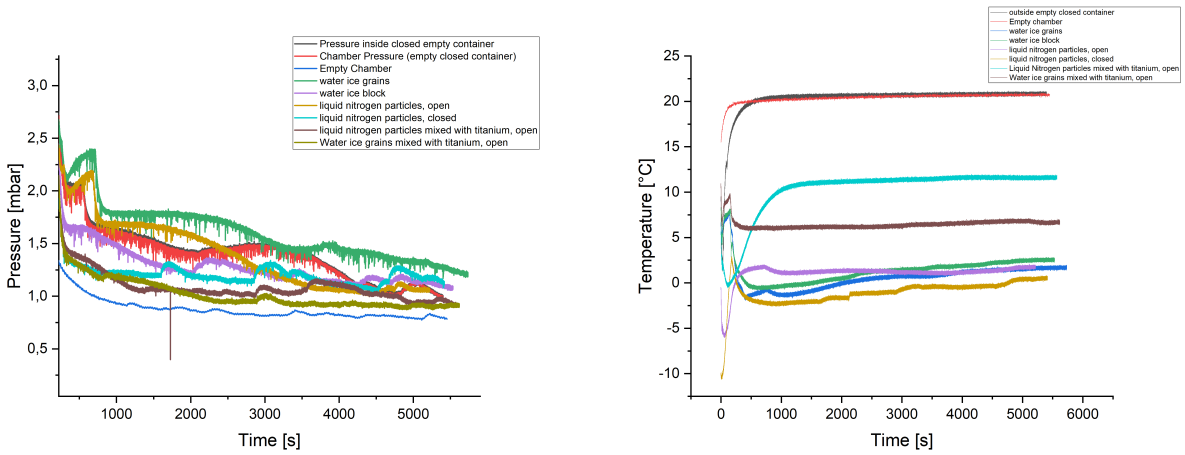

(a) Pressure on ice surface during the entire duration of the experiments.

(b) Temperature on ice surface during the entire duration of the experiments.

Figure D.2: Pressure and Temperature during the second set of experiments

When liquid nitrogen ice particles are mixed with titanium, more sublimation seems to happen then when water ice grains are combined. This is however only caused by the titanium that due to the pressure is ejected within the vacuum chamber.

Moreover, when comparing the experiments of the two sets in Figures D.2 and D.3, regarding water ice grains mixed with titanium, it is seen how much the temperature of titanium powder influences the results. When it is as cold as the ice, the water ice sublimation is way more difficult then when TiO_2 is at room temperature.

In Figure D.3, not considering the first three experiments with the empty chamber (which were done in order to start up the chamber, at the beginning of the day), it is shown that when adding titanium to the mix, the sublimation of water is way less, the pressure in the chamber is around 1 mbar rather than 1.5 mbar, that, instead, happens when no TiO_2 is present.

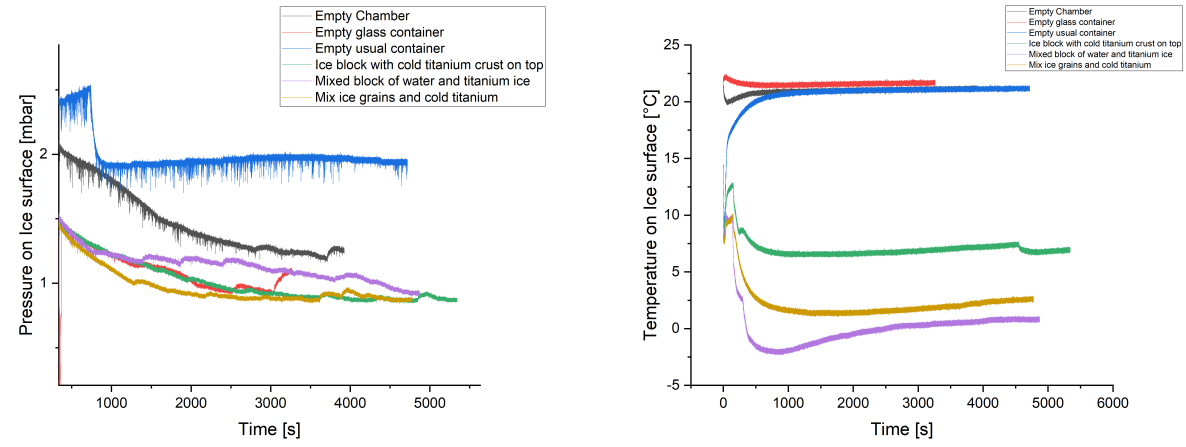

(a) Pressure on ice surface during the entire duration of the experiments.

(b) Temperature on ice surface during the entire duration of the experiments.

Figure D.3: Pressure and Temperature during the third set of experiments

Bibliography

Alan May R., B. K. D., Scott Smith R. (2013a). The release of trapped gases from amorphous solid water films. i."top-down" crystallization-induced crack propagation probed using the molecular volcano. *The Journal of Chemical Physics*, *138*(10), 104501.

Alan May R., B. K. D., Scott Smith R. (2013b). The release of trapped gases from amorphous solid water films. ii."bottom-up" induced desorption pathways. *The Journal of Chemical Physics*, *138*(10), 104502.

Ayotte, P., Smith, R. S., Stevenson, K. P., Dohnálek, Z., Kimmel, G. A., & Kay, B. D. (2001). Effect of porosity on the adsorption, desorption, trapping, and release of volatile gases by amorphous solid water. *Journal of Geophysical Research: Planets*, *106*(E12), 33387–33392.

Biver, N., Bockelee-Morvan, D., Colom, P., Crovisier, J., Davies, J. K., Dent, W. R., Despois, D., Gerard, E., Lellouch, E., Rauer, H., et al. (1997). Evolution of the outgassing of comet hale-bopp (c/1995 o1) from radio observations. *Science*, *275*(5308), 1915–1918.

Biver, N., Bockelée-Morvan, D., Colom, P., Crovisier, J., Germain, B., Lellouch, E., Davies, J., Dent, W., Moreno, R., Paubert, G., et al. (1997). Long-term evolution of the outgassing of comet hale-bopp from radio observations. *Earth, Moon, and Planets*, *78*(1), 5–11.

Biver, N., Bockelée-Morvan, D., Colom, P., Crovisier, J., Henry, F., Lellouch, E., Winnberg, A., Johansson, L. E., Gunnarsson, M., Rickman, H., et al. (2002). The 1995–2002 long-term monitoring of comet c/1995 o1 (hale-bopp) at radio wavelength. *Cometary science after hale-bopp* (pp. 5–14). Springer.

Bockelée-Morvan, D., Crovisier, J., Mumma, M., & Weaver, H. (2004). The composition of cometary volatiles. *Comets Ii*, *1*, 391–423.

Breithaupt, J. (2000). New understanding physics for advanced level.

Brown, W. A., & Bolina, A. S. (2007). Fundamental data on the desorption of pure interstellar ices. *Monthly Notices of the Royal Astronomical Society*, *374*(3), 1006–1014.

Buratti, B. J., Choukroun, M., & Bauer, J. M. (2016). The low albedo of comets. *AGU Fall Meeting Abstracts*, P43A–2083.

Collings, M. P., Anderson, M. A., Chen, R., Dever, J. W., Viti, S., Williams, D. A., & McCoustra, M. R. (2004). A laboratory survey of the thermal desorption of astrophysically relevant molecules. *Monthly Notices of the Royal Astronomical Society*, *354*(4), 1133–1140.

Combi, M. R., Harris, W. M., & Smyth, W. H. (2004). Gas dynamics and kinetics in the cometary coma: Theory and observations. *Comets II*, *1*, 523–552.

David, K., Gorham, J., Kim, S., Miller, P., & Minkus, C. (2006). Aeronautical wind tunnels, europe and asia.

De Pater, I., & Lissauer, J. J. (2015). *Planetary sciences*. Cambridge University Press.

Festou, M., Keller, H. U., & Weaver, H. A. (2004). *Comets ii*. University of Arizona Press.

Gálvez, Ó., Maté, B., Herrero, V. J., & Escribano, R. (2009). Spectroscopic effects in ch4/h2o ices. *The Astrophysical Journal*, *703*(2), 2101.

Gundlach, B., Skorov, Y. V., & Blum, J. (2011). Outgassing of icy bodies in the solar system–i. the sublimation of hexagonal water ice through dust layers. *Icarus*, *213*(2), 710–719.

Hansen, K. C., Altwegg, K., Berthelier, J.-J., Bieler, A., Biver, N., Bockelée-Morvan, D., Calmonte, U., Capaccioni, F., Combi, M., De Keyser, J., et al. (2016). Evolution of water production of 67p/churyumov–gerasimenko: An empirical model and a multi-instrument study. *Monthly Notices of the Royal Astronomical Society*, *462*(Suppl_1), S491–S506.

He, J., Emtiaz, S., & Vidali, G. (2018). Measurements of diffusion of volatiles in amorphous solid water: Application to interstellar medium environments. *The Astrophysical Journal*, *863*(2), 156.

Herrero, V. J., Gálvez, Ó., Maté, B., & Escribano, R. (2010). Interaction of ch 4 and h 2 o in ice mixtures. *Physical Chemistry Chemical Physics*, *12*(13), 3164–3170.

Jambon-Puillet, E., Shahidzadeh, N., & Bonn, D. (2018). Singular sublimation of ice and snow crystals. *Nature communications*, *9*(1), 1–6.

Jenniskens, P., & Blake, D. (1996). Crystallization of amorphous water ice in the solar system. *The astrophysical journal*, *473*(2), 1104.

Jenniskens, P., Blake, D., Wilson, M., & Pohorille, A. (1995). High-density amorphous ice, the frost on interstellar grains. *The Astrophysical Journal*, *455*, 389.

Jenniskens, P., & Blake, D. F. (1994). Structural transitions in amorphous water ice and astrophysical implications. *Science*, *265*(5173), 753–756.

Kaufmann, E., Kargl, G., Kömle, N. I., Steller, M., Hasiba, J., Tatschl, F., Ulamec, S., Biele, J., Engelhardt, M., & Romstedt, J. (2009). Melting and sublimation of planetary ices under low pressure conditions: Laboratory experiments with a melting probe prototype. *Earth, Moon, and Planets*, *105*(1), 11–29.

Kossacki, K. J. (2021). Sublimation of porous granular ice in vacuum. *Icarus*, *368*, 114613.

Kossacki, K. J., Leliwa-Kopystynski, J., Witek, P., Jasiak, A., & Dubiel, A. (2017). Sublimation of cometary ices in the presence of organic volatiles. *Icarus*, *294*, 227–233.

Krause, M., Blum, J., Skorov, Y. V., & Trieloff, M. (2011). Thermal conductivity measurements of porous dust aggregates: I. technique, model and first results. *Icarus*, *214*(1), 286–296.

Lewis, D., & Gladstone, S. (1960). *Elements of physical chemistry*. Princeton, NJ.

Luna, R., Satorre, M., Santonja, C., & Domingo, M. (2014). New experimental sublimation energy measurements for some relevant astrophysical ices. *Astronomy & Astrophysics*, *566*, A27.

Marboeuf, U., Schmitt, B., Petit, J.-M., Mousis, O., & Fray, N. (2012). A cometary nucleus model taking into account all phase changes of water ice: Amorphous, crystalline, and clathrate. *Astronomy & Astrophysics*, *542*, A82.

Martín-Doménech, R., Caro, G. M., Bueno, J., & Goesmann, F. (2014). Thermal desorption of circumstellar and cometary ice analogs. *Astronomy & Astrophysics*, *564*, A8.

Mastrapa, R., Sandford, S., Roush, T., Cruikshank, D., & Dalle Ore, C. (2009). Optical constants of amorphous and crystalline h2o-ice: 2.5–22 μm (4000–455 cm- 1) optical constants of h2o-ice. *The Astrophysical Journal*, *701*(2), 1347.

Maté, B., Cazaux, S., Satorre, M. Á., Molpeceres, G., Ortigoso, J., Millán, C., & Santonja, C. (2020). Diffusion of ch4 in amorphous solid water. *Astronomy & Astrophysics*, *643*, A163.

Maté, B., Medialdea, A., Moreno, M. A., Escribano, R., & Herrero, V. J. (2003). Experimental studies of amorphous and polycrystalline ice films using ft-rairs. *The Journal of Physical Chemistry B*, *107*(40), 11098–11108.

Minissale, M., Aikawa, Y., Bergin, E., Bertin, M., Brown, W. A., Cazaux, S., Charnley, S. B., Coutens, A., Cuppen, H. M., Guzman, V., et al. (2022). Thermal desorption of interstellar ices: A review on the controlling parameters and their implications from snowlines to chemical complexity. *ACS Earth and Space Chemistry*, *6*(3), 597–630.

Mispelaer, F., Theulé, P., Aouididi, H., Noble, J., Duvernay, F., Danger, G., Roubin, P., Morata, O., Hasegawa, T., & Chiavassa, T. (2013). Diffusion measurements of co, hnco, h2co, and nh3 in amorphous water ice. *Astronomy & Astrophysics*, *555*, A13.

Moores, J., Brown, R., Lauretta, D., & Smith, P. (2006). Sublimation of water ice in low pressure environments: Isotopic effects and implications for the martian paleoclimate record. *Fourth International Conference on Mars Polar Science and Exploration*, *1323*, 8031.

Pat-El, I., Laufer, D., Notesco, G., & Bar-Nun, A. (2009). An experimental study of the formation of an ice crust and migration of water vapor in a comet's upper layers. *Icarus*, *201*(1), 406–411.

Rubin, M., Engrand, C., Snodgrass, C., Weissman, P., Altwegg, K., Busemann, H., Morbidelli, A., & Mumma, M. (2020). On the origin and evolution of the material in 67p/churyumov-gerasimenko. *Space science reviews*, *216*(5), 1–43.

Schrijer, F. F., & Bannink, W. J. (2010). Description and flow assessment of the delft hypersonic ludwieg tube. *Journal of Spacecraft and Rockets*, *47*(1), 125–133.

Sklavenitis, S. (2022). *Experimental simulation and assessment of the geysers of icy moons in the laboratory* (Doctoral dissertation). Delft University of Technology.

Snodgrass, C., Opitom, C., de Val-Borro, M., Jehin, E., Manfroid, J., Lister, T., Marchant, J., Jones, G. H., Fitzsimmons, A., Steele, I. A., et al. (2016). The perihelion activity of comet 67p/churyumov–gerasimenko as seen by robotic telescopes. *Monthly Notices of the Royal Astronomical Society*, *462*(Suppl_1), S138–S145.

Stern, S. A., Colwell, W. B., Festou, M. C., Tamblyn, P. M., Parker, J. W., Slater, D. C., Weissman, P. R., & Paxton, L. J. (1999). Comet hale-bopp (c/1995 o1) near 2.3 au postperihelion: Southwest

ultraviolet imaging system measurements of the h2o and dust production. *The Astronomical Journal*, *118*(2), 1120.

Strazzulla, G. (1999). Ion irradiation and the origin of cometary materials. *Composition and Origin of Cometary Materials*, 269–274.